Short title: Gene expression in cowpea reproductive cell-types.

Author for Contact: Anna M.G. Koltunow

Article title:

Gene expression in isolated cowpea (Vigna unguiculata L. Walp) cells from meiosis to seed initiation

Author names and affiliations:

Nial Gursanscky[1], Danielle Mazurkiewicz[1], Martina Juranić[1], Susan D. Johnson[1], Gloria León[2], Rocio Escobar-Guzmán[2], Rigel Salinas-Gamboa[2], Itzel Amasende-Morales[2], Matteo Riboni[1], Melanie Hand[1], Andrew Spriggs[3], Jean-Philippe Vielle-Calzada[2] and Anna M.G. Koltunow[1,4]

1: Commonwealth Scientific and Industrial Research Organisation (CSIRO) Agriculture and Food, Waite Campus, Urrbrae, South Australia 5064, Australia

2: Group of Reproductive Development and Apomixis, UGA Laboratorio Nacional de Genómica para la Biodiversidad, CINVESTAV Irapuato, Guanajuato 36821, México.

3: CSIRO Agriculture and Food, Black Mountain Science and Innovation Park, Canberra, ACT 2601, Australia.

Author Contributions:

D.M. isolated LCM cell types, and obtained transcriptomes; N.G. conducted data analyses identifying expression profiles and developmental trends; M.J. and S.D.J. contributed to cell cycle and transgenic cowpea analyses; G.L., R.E-G and R.S-G. performed *in situ* hybridizations; M.R verified gene expression by qRT-PCR; M.H. prepared constructs; I.A-M.

carried out promoter characterization in *Arabidopsis*; A.S. assembled transcriptomes, carried out global alignments of RNA-seq to genomic sequences ; J-P.V-C. and A.M.G.K. designed experiments and analyzed data. N.G., J-P.V-C. and A.M.G.K wrote the paper. A.M.G.K. agrees to serve as the author responsible for contact and ensures communication.

Funding information: This work was funded by a grant from the Bill and Melinda Gates foundation to the Commonwealth Scientific and Industrial Research Organisation (CSIRO) (OPP1076280).

Present address:

[4.] Queensland Alliance for Agriculture and Food Innovation (QAAFI) Centre for Crop Science. The University of Queensland. St Lucia. Queensland 4072. Australia.

Email address of author for contact: a.koltunow@uq.edu.au

One sentence summary

Analyses of laser capture derived cell-type transcriptomes spanning meiosis to seed initiation revealed gene expression profiles during cell specification and reproductive development in cowpea.

Abstract

Molecular knowledge of pathways regulating seed formation in legumes, remains scarce. Thirteen isolated cell-type transcriptomes were developed, spanning temporal events of male and female gametogenesis and seed initiation, to examine pathways involved in

cowpea seed formation. *In situ* hybridization confirmed localization of *in silico* identified cell-specific genes, verifying transcriptome utility. Cowpea and *Arabidopsis* reproductive cells showed some conservation in regulators enabling cell-type expression as some cowpea cell-specific genes promoters and their *Arabidopsis* homologs directed expression to identical reproductive cell-types in transgenic plants. *In silico* analyses revealed gene expression similarities and differences with genes in pathways regulating reproductive events in other plants. Meiosis-related genes were expressed at mitotic stages of gametogenesis and during sporophytic development in cowpea. Plant hormone pathways showing preferential expression at particular reproductive stages were identified. Expression of epigenetic pathways, resembling those found in *Arabidopsis,* including microRNA mediated gene silencing, RNA directed DNA methylation and histone modification were associated with particular stages of male and female gametophyte development, suggesting roles in gametogenic cell specification and elaboration. Analyses of cell-cycle related gene expression in mature cowpea female gametophytes, indicated that the egg and central cell were arrested at the G1/S and G2/M cell cycle phases, respectively, prior to fertilization. Pre-fertilization female gametophyte arrest was characterized by barely detectable auxin biosynthesis gene expression levels, and elevated expression of genes involved in RNA-mediated gene silencing and histone modification. These transcriptomes provide a useful resource for additional interrogation to support functional analyses for development of higher yielding cowpea and syntenic legume crops.

Introduction

Legumes contribute directly and indirectly to world food supply. Higher in protein, they provide forage for animals and increase soil fertility by fixing nitrogen. Agronomic

70 improvement of eight grain legumes, including cowpea (*Vigna unguiculata* L. Walp) has
71 been targeted by the Consultative Group for International Agricultural Research
72 (https://storage.googleapis.com/cgiarorg/2018/11/SC7-B_Breeding-Initiative-1.pdf). We
73 aim to increase seed yield and quality in cowpea, which originated in Africa and remains an
74 important subsistence crop in sub-Saharan Africa (Singh, 2014). Although cowpea is
75 relatively tolerant to drought, it is prone to high levels of flower and pod drop, resulting in
76 decreased seed yields. There is limited knowledge of the molecular pathways supporting
77 successful elaboration of cowpea male and female gametophytes and seeds.
78
79 Current genomic resources for cowpea include a reference genome (Lonardi et al., 2019,
80 Munoz-Amatriain et al., 2017) together with survey genomes and transcriptomes from
81 various plant tissues (Spriggs et al., 2018, Yao et al., 2016). Reproductive events occur only
82 in a few cell-types buried within cowpea floral organs (Salinas-Gamboa et al., 2016).
83 Therefore, laser capture microdissection (LCM) is a useful approach to isolate reproductive
84 cell-types to generate informative transcriptomes. Interrogation of these reproductive cell-
85 type transcriptomes in conjunction with cowpea genome and tissue transcriptome
86 resources could accelerate identification and functional examination of pathways
87 supporting successful cowpea seed formation.
88
89 A cowpea reproductive calendar has been developed linking morphological floral features in
90 cowpea to reproductive events in floral tissues to support collection of tissues for molecular
91 analyses (Salinas-Gamboa et al., 2016). Male gametophyte precursor cells, termed pollen
92 mother cells (PMC) undergo meiosis (sporogenesis) forming tetrads of microspores (mTET)
93 in the anther. Individual microspores (MIC) then undergo mitosis (microgametogenesis) and

differentation to form the mature pollen grain (MP-SC) containing a generative and a vegetative cell (Fig. 1A). By contrast, during female gametophyte development, a single megaspore mother cell (MMC) in each ovule undergoes meiosis to form a tetrad of megaspores (fTET). Three megaspores degenerate and the surviving functional megaspore (FM) undergoes three rounds of mitosis to form a syncytium of eight nuclei (megagametogenesis). Cellularization events result in a 7-celled *Polygonum*-type female gametophyte, or embryo sac, and three of these degrade. The mature cowpea embryo sac (MES) contains an egg cell (EC) progenitor of the embryo (Em), flanked by two synergids (Sy), which guide fertilization events and the central cell (CC) containing two fused haploid nuceli, which is the progenitor of the endosperm (En; Fig. 1A; Salinas-Gamboa et al., 2016).

The events of fertilization initiate with pollen grain germination and emergence of the pollen tube on the stigma. We have observed that mitosis of the generative cell to form the two sperm cells predominantly occurs after pollen tube germination (see Results). Pollen tube growth through maternal tissues into the ovule, synergid puncture and pollen tube burst releases both sperm cells into the embryo sac. One sperm cell fuses with the egg to initiate embryogenesis and the other fuses with with the polar nucleus of the central cell to produce the triploid endosperm. Endosperm tissue is transient in copwpea as it is utilized during embryo development (Salinas-Gamboa et al., 2016); Fig. 1A).

Studies in *Arabidopsis*, rice, maize, *Boechera* and *Hieracium* have used LCM to isolate cells involved in sexual and asexual (apomictic) reproductive events to examine cell-type specific gene expression (Anderson et al., 2013, Kubo et al., 2013, Zhan et al., 2015, Belmonte et al., 2013, Okada et al., 2013). These analyses have typically focused on the expression in cells

118 involved in specific aspects of the reproductive pathway due to the biological questions
119 being addressed, and potentially, the laborious nature of the method. To our knowledge, a
120 transcriptome series spanning reproductive events in isolated cells from the initiation of
121 meiosis to seed initiation has not been generated in a species. This would enable direct
122 comparisons of gene expression during male and female gametogenesis and seed
123 development within the plant and also with pathways known to functionally regulate cell
124 specification and reproductive development in other plants.
125
126 Here, we used LCM and additional tissue isolation procedures, to develop a suite of 13
127 cowpea reproductive cell-type transcriptomes spanning the temporal events of male and
128 female gametophyte development, and early seed initiation in cowpea. *In vitro* and *in*
129 *planta* analyses were used to verify transcriptome integrity. Following an analysis of global
130 gene expression profiles across the transcriptome set, an *in silico* analysis of the expression
131 of genes involved in epigenetic regulation, hormone biosynthesis and signal transduction,
132 and cell cycle progression was undertaken as these pathways regulate reproductive aspects
133 in other angiosperms. These analyses revealed commonalities between cowpea and other
134 species with respect to some of these pathways, in addition to novel cowpea-related
135 differences identifying genes and pathways as candidates for future functional testing.

136 **Results**

137 **Cowpea IT86D-1010 leaf and reproductive cell-type transcriptomes and PCR verifications**
138 A total of 13 reproductive transcriptomes were generated, in duplicate, using RNA extracted
139 from individual reproductive cells that span male and female gametogenesis, and early seed
140 initiation. Laser capture microdissection was used to generate 12 reproductive cell-type

141 transcriptomes, while pollen and sperm cells were sampled separately (see below, Fig. 1A).
142 Female gametophyte-related cell-type transcriptomes were generated for the megaspore
143 mother cell (MMC) during meiosis I, the tetrad of post-meiotic megaspores (fTET),
144 developing mitotic embryo sacs with two or four nuclei (ES2n, ES4n), and the mature
145 embryo sac (MES) containing the egg cell (EC), the flanking synergids (Sy), and the central
146 cell (CC), at the time of stamen emergence (anthesis). Individual EC and CC transcriptomes
147 were also made. The early embryo (Em) transcriptome comprised tissue from developing
148 zygotes to early globular stages of cowpea embryogenesis (Fig 1A).
149
150 Male gametophyte-related transcriptomes were generated for pollen mother cells at early
151 and later stages of meiosis I (PMC.E, PMC.L), microspore tetrads (mTET), and uninucleate
152 microspores (MIC). A pure sperm cell transcriptome was not generated. Analyses of cleared
153 anthers indicated that 9.7% of mature pollen grains contained two sperm cells (n=500),
154 indicating the final generative cell mitosis giving rise to the sperm cells primarily occurs
155 following pollen tube germination. This is also observed in soybean and 70% of flowering
156 plant species (Brewbaker, 1967, Williams et al., 2014, Haerizadeh et al., 2009,
157 Wojciechowski et al., 2004). Anthers and pistils harvested at anthesis were processed to
158 create a transcriptome referred to as mature pollen-sperm cell (MP-SC; see Methods for
159 details). An additional transcriptome generated from young expanding cowpea leaves
160 served as a control comparison for gene expression in cells not undergoing reproductive
161 events.
162
163 A total of 74,839 genes were predicted in the IT86D-1010 genome (Spriggs et al., 2018)
164 using Augustus gene prediction software when *Arabidopsis* genes were used as the training

data set (Supplemental Data 1). Transcriptome sequences were aligned with the predicted genes in the IT86D-1010 cowpea genome to identify common and uniquely expressed genes across all datasets (Supplemental Table 1, Supplemental Data 2). The total number of uniquely expressed genes within each transcriptome ranged from 22,561 in the female megaspore tetrad (fTET) to 60,359 in the MP-SC sample (Fig. 1B). Only 3,769 of the genes expressed in the MP-SC transcriptome were not detected in at least one other cell-type. As a likely consequence of its isolation method, the high transcript diversity in the MP-SC transcriptome contrasts with that found in pollen and sperm cell transcriptomes of *Arabidopsis*, rice and maize, where the number of genes detected is reduced compared to sporophytic cell-types (Rutley and Twell, 2015).

Gene expression across all of the transcriptomes was normalized using reads per million (RPM) given the absence of a correlation between gene length and read alignment number. Investigation of unique gene expression levels within each transcriptome indicated that the majority of unique genes (68-85%) were expressed at very low to moderate levels (<1 to 5-20 RPM; Fig 1C). Principal component analysis (PCA) using the individual transcriptome replicates showed that most replicates clustered together. The transcriptomes from male and female reproductive cell-types co-segregated forming two distinct male and female clusters. The embryo transcriptomes associated with the female reproductive transcriptome cluster, while the leaf and MP-SC transcriptomes were outliers (Supplemental Fig.2).

The quality of the generated transcriptomes was evaluated by examining if cell-type specific genes could be identified via *in silico* methods in the transcriptomes, and then by verifying gene expression by qRT-PCR, *in situ* and transgenic approaches. Candidate cell-type specific

189 genes were initially identified using rsgcc software in the MMC, PMC, EN2n, En4n, MES, CC,
190 ES, Em and sperm transcriptomes (Fig. 1A). Candidate genes identified ranged in number
191 from 126 in early pollen mother cells to 25,986 in the MP-SC transcriptome (Supplemental
192 Data 3 and 4). A filtering approach based on identification of genes expressed at least five
193 times higher in the CC, EC or MP-SC transcriptomes relative to all others resulted in 10, 34
194 and 31 candidate specific genes, respectively (Supplemental Table 2).
195
196 Two of the cowpea egg cell-specific candidates identified using the filtering approach were
197 homologues of the *Arabidopsis* egg cell-specific genes *AtEC1.1*, (Sprunck et al., 2012) and
198 *AtRKD1* (Koszegi et al., 2011) (*VuEC1.1_1* and *VuRKD1*; Table 1). Therefore, cowpea
199 homologues of 11 additional *Arabidopsis* reproductive cell-type expressed genes were
200 identified for verification analyses. They included *VuKNU-like1* and *2*, putative cowpea
201 homologs of the *Arabidopsis KNUCKLES* gene expressed during male and female
202 gametogenesis (Payne et al., 2004, Tucker et al., 2012) and genes expressed in specific male
203 and female gametophytic cell-types (Table 1; Supplemental Table 3). Twenty of the 28 (71%)
204 candidate cell-type specific genes tested by qRT-PCR, were confirmed as significantly
205 enriched using cDNA isolated from tissues at comparable developmental stages from which
206 the LCM samples were obtained in addition to other tissue types (Table 1, Supplemental
207 Table 4).
208
209 **Verification of cell-type specific expression using *in situ* hybridization and plant**
210 **transformation**
211 The expression of 11 candidate cell-type specific genes verified using qRT-PCR analyses
212 above was examined by *in situ* hybridization (ISH), using gene-specific digoxygenin-labelled

213 probes (Fig. 2 and Supplemental Fig. 4). ISH was performed on mature pollen grains to
214 examine expression of four candidate sperm-cell specific genes, as we had previously
215 determined that approximately 10 percent of mature pollen grains contain two sperm cells
216 (Table 1). *VuXTH6* mRNA was detected at high levels in the sperm cells and in the vegetative
217 nucleus, with low levels detected in the vegetative cell cytoplasm (Fig. 2A-C). By contrast,
218 mRNA for the other three examined genes was detected in the sperm cells, the vegetative
219 nucleus and at high levels in the vegetative cell cytoplasm (Fig. 2D-F and Supplemental Fig.
220 4A-F).
221
222 A combination of whole-mount and section-based *in situ* hybridization was used in
223 developing cowpea ovules used to examine expression of seven genes during female
224 gametogenesis. Transcripts of *VuKNU-like1*, the candidate cowpea homolog of the
225 *Arabidopsis KNUCKLES* gene were enriched in the megaspore mother cell; however,
226 expression was also observed in nucellar and inner integumentary ovule cells (Fig 2G).
227 Transcripts from the candidate egg cell specific *VuEC1.1_1* and *VuRKD1* genes (Table 1) were
228 highly enriched in the egg cell, in comparison to the rest of the embryo sac and ovule. In
229 both cases, mRNA localization was also evident in the synergids, but not in the central cell
230 (Fig. 2H; Supplemental Fig. 4G-J). Three of the four candidate central cell genes tested by *in*
231 *situ* hybridization, displayed specific mRNA localization in the central cell (*VuSDR1,*
232 *VuGULL06*; Table 1; Supplemental Fig. 4N and O, Fig 2I). *VuNB-ARC*, mRNA was evident in a
233 nuclear dot patterning in the cowpea central cell nucleus (Fig. 2I). Nuclear dots are tightly
234 associated with nascent transcripts of actively expressed genes in the central cell of
235 *Arabidopsis* (Vielle-Calzada et al., 1999), and in embryonic cells of *Drosophila melanogaster*

(Shermoen and O'Farrell, 1991). *VuMEE23* mRNA was localized in the central cell and in adjacent ovule cells (Table 1).

As eleven of the cowpea genes predicted to be expressed in specific reproductive cell- types showed sequence similarity to previously described *Arabidopsis* cell-type expressed genes, cowpea plants were transformed with constructs comprising *Arabidopsis* (*At*) promoters of these genes fused to fluorescent reporters to examine conservation of targeting to specific reproductive cell-types (Table 1; Supplemental Table 3). Six of the tested promoters directed similar spatial and temporal patterns in cowpea as observed in *Arabidopsis*. The remaining five showed either non-specific or no detectable expression in transgenic cowpea (Table 1; Fig. 2 and Supplemental Fig. 4). The *AtKNU* promoter directed expression to the MMC and PMC cells, as published previously (Tucker et al., 2012) but expression was also evident in the chalazal region of the cowpea ovule integument (Supplemental Fig. 5F). *In situ* hybridization using probes to detect native cowpea *VuKNU* expression confirmed expression in the ovule integument (Supplemental Fig.4K). The *AtDD45* promoter directed expression to the egg cell (Fig. 2J) and both *AtDD9* and *DD25* promoters enabled central cell expression (Fig. 2K). The *AtEC1.1* and *RKD2* promoters directed reporter expression to egg cells of transgenic cowpea (Fig. 2K-M). Expression of fluorescent reporters from *AtRKD2* and *DD45* promoters was also observed in early cowpea embryos (Fig. 2N-O).

Given the low efficiency and lengthy nature of the cowpea transformation protocol used, we also examined if upstream promoter regions of 11 of the cowpea candidate cell-type specific genes identified from *in silico* analyses would direct the same cell-type expression in *Arabidopsis*. Genomic fragments of 0.8 to 3.2 kb, corresponding to their upstream putative

promoter regions were fused to the *uidA* (GUS) reporter gene and transformed into the *Arabidopsis* Columbia (*Col*-0) ecotype. For each transcriptional fusion, at least 15 independent transformants were recovered and histologically analyzed to examine gene expression patterns during male and female gametogenesis. GUS activity was not detected in reproductive organs of *Arabidopsis* in seven of the 11 tested constructs. However, a 1,429 bp region upstream of *VuKNU-L1* drove GUS expression in the *Arabidopsis* MMC and adjacent sporophytic ovule cells, in a pattern similar to the *VuKNU-L1* mRNA ISH localization pattern in cowpea (Supplemental Fig. 6A and Supplemental Table 21). The promoter fragments from the *pVuXTH32* and *pVuGIM2* genes drove spatial expression in both pollen sperm and vegetative cells as observed in cowpea ISH experiments (Supplemental Fig. 6F-G). By contrast, the promoter of *pVuRKD1* drove expression in the egg cell, and in both sperm and vegetative cells in 5 of the 15 *Arabidopsis* transformants analyzed (Supplemental Fig. 6B-D). In seven of the transformants, expression was seen only in sperm cells (Supplemental Fig. 6C). Finally, the promoter of the cowpea gene *VuGULL06*, a candidate selected for potential central cell expression drove expression in the *Arabidopsis* egg cell and synergids (Supplemental Fig. 6E), suggesting that in some cases cowpea promoters can be influenced by heterologous factors intrinsic to the *Arabidopsis* genome.

The promoter analyses indicated that there is some conservation in regulators enabling reproductive cell-type specific expression in cowpea and Arabidopsis given the conservation of gene expression directed to common cell types in transgenic studies, in some cases. Taken together, these verification analyses collectively indicted that the developed transcriptomes were a reliable resource for further *in silico* interrogation of gene expression

283 profiles defining specific reproductive cell-types during male and female gametogenesis and
284 early cowpea embryogenesis.

285 **Enriched biological processes in cowpea reproductive transcriptomes**

286

287 Differentially expressed (DE) genes were identified in each transcriptome type to examine
288 gene expression changes occurring during the temporal events of male and female
289 gametogenesis and early embryogenesis (Supplemental Data 4). Percentages of
290 differentially expressed genes varied widely from 3.4% to 25% amongst the transcriptomes
291 (Supplemental Table 5). Comparisons between the cowpea female reproductive cell-type
292 transcriptomes generated using LCM and those previously generated using LCM in
293 *Arabidopsis* revealed low levels of common genes. Comparisons were made between the
294 cowpea data set and those generated in *Arabidopsis* for the MMC (Schmidt et al., 2011),
295 ovule nucellus, early mitotic female gametophytes (Tucker et al., 2012) and the egg and
296 central cell (Wuest et al., 2010, Steffen et al., 2007). The highest similarity, with a 24%
297 overlap, was observed between the cowpea MMC dataset and the *Arabidopsis* female
298 nucellus plus MMC data set (Tucker et al., 2012); Supplemental Table 6). The low levels of
299 common genes observed may reflect differences in species-specific genes, staging, and
300 methods used to generate transcriptomes and identify expressed genes.

301

302 To obtain an overview of the major biological processes occurring during gametogenesis and
303 seed initiation, each transcriptome was initially surveyed by examining significantly enriched
304 gene ontology (GO) terms in the biological processes' category (Fig. 3A- B). Examination of
305 the control expanding leaf transcriptome showed that it was, unsurprisingly, enriched in GO

306 terms related to light transduction, chlorophyll, photosynthesis, and sugar metabolism (Fig.
307 3). Each cowpea reproductive transcriptome was characterized by a relatively distinct set of
308 significantly enriched biological process terms, supporting the cytologically distinct nature of
309 the cell-types collected (Fig. 3A-B).
310
311 Meiosis and recombination, and cell wall biogenesis terms, which characterize the
312 functional and cytological events of male and female sporogenesis in angiosperms, were
313 found in cowpea meiotic cell transcriptomes. Terms related to a range of pathways involved
314 in epigenetic regulation were also prevalent in transcriptomes related to the elaboration of
315 the female and male gametophytes (Fig. 3A-B). Regulation by small RNAs and global
316 changes in DNA and histone methylation modifications influence determination, selection
317 and development of gametophytic cells (Tucker et al., 2012, Olmedo-Monfil et al., 2010).
318 They prevent transposon activation during male and female gametogenesis (Slotkin et al.,
319 2009, Schoft et al., 2011, Pillot et al., 2010, Ibarra et al., 2012, Martinez et al., 2016). In
320 *Arabidopsis*, Histone H3 methylation (at lysine (K) 27) by the *Polycomb*-Group protein
321 repressive complex 2 (PRC2), results in gene silencing and regulates *Arabidopsis* male
322 gametophyte formation and female gametophyte arrest, pre-fertilization (Mozgova and
323 Hennig, 2015, Grossniklaus and Paro, 2014, Wang and Kohler, 2017, Kawashima and Berger,
324 2014).
325
326 The plant hormone auxin is involved in a range of reproductive events in angiosperms,
327 including initiation of seed formation and embryo patterning. Auxin-related terms were very
328 evident in this global analysis. Interestingly, the GO enrichment analysis suggested potential
329 involvement of other plant hormone pathways at particular cowpea developmental stages.

For example, the abscisic acid signalling pathway featured in the female MMC and male late PMC transcriptomes. Brassinosteroid-related terms were evident in dividing embryo sacs with 2 and 4 nuclei, and terms related to jasmonic acid biosynthetic processes and responses to cytokinin were evident in the mature cowpea embryo sac (Fig. 3A and Supplemental Data 6).

In order to gain greater understanding of reproduction-related gene expression pathways that cowpea may, or may not have in common with other angiosperms, we profiled the transcriptome set for the expression of cowpea homologues of *Arabidopsis* genes involved in meiosis, auxin biosynthesis and signal transduction, epigenetic pathways and cell-cycle progression. The results of these analyses, in the sections below, collate examined gene expression profiles during male and female gametogenesis, pre-fertilization female gametophyte arrest and early embryogenesis.

Gene expression during temporal events of cowpea male gametophyte formation

The expression of 18 cowpea meiosis-related gene homologues during male gametogenesis is shown in Fig. 3C. The profiled genes have putative functions in chromosome pairing, homologous recombination, and subsequent meiotic events (see Supplemental Table 7 for functional information and references). A number of these genes were clearly expressed in non-meiotic cell-type transcriptomes and in leaf (Fig. 3C), consistent with expression data from other species (Klepikova et al., 2016).

Analyses of the expression of 276 auxin biosynthesis and signal transduction pathway genes in male gametogenesis showed high levels of the cowpea *YUCCA6*-like auxin biosynthesis

354 gene in transcriptomes of cowpea late pollen mother cells, tetrads and microspores (Fig. 4A,
355 Supplemental Table 9). This reflects the requirement of *YUCCA6* and auxin production in
356 corresponding cells for viable *Arabidopsis* pollen development (Yao et al., 2018). Cowpea
357 homologs of the *Arabidopsis ARF19*, *AIR12* and *DRB1* auxin-responsive genes were also
358 upregulated during male gametophyte formation (Fig 4B). In *Arabidopsis*, ARF19 enables
359 auxin-activated transcriptional responses to phosphate starvation (Huang et al., 2018).
360 AIR12 is thought to link auxin signal transduction and reactive oxygen signalling (Gibson and
361 Todd, 2015) and DRB1 is involved in cleavage to produce miR399 phosphate homeostasis
362 regulation (Pegler et al., 2019).
363
364 Cowpea *ARGONAUTE* (*AGO*) genes were identified because AGO proteins are central to the
365 small RNA-mediated processes of Post-transcriptional Gene Silencing (PTGS), microRNA
366 (miRNA) mediated gene silencing and RNA-directed DNA methylation (RdDM). The 13
367 cowpea *AGO*-like genes identified showed close phylogenetic relationships with known
368 *AGOs* in other plants, although *AGO8* and *AGO9* were not evident in the cowpea genome
369 (Supplemental Fig. 7).
370
371 Analyses of cowpea homologs of genes required for the 21 nt producing *Arabidopsis*
372 microRNA pathway showed that *AGO1*, *HEN1*, *HYL1* and *HST1* were co-expressed during
373 meiotic and mitotic stages of male gametophyte development. This suggested potential
374 conservation of this pathway with a functional role during cowpea male gametophyte
375 elaboration (Fig. 6A).
376

377 By contrast, the case for a functional *Arabidopsis*-like PTGS pathway operating during male
378 gametogenesis appeared doubtful. The *Arabidopsis* PTGS pathway typically produces 21-24
379 nt small interfering (si) RNAs. It requires the function of AGO1, RDR6, SGS3 and DCL4 as core
380 protein components. However, AGO2, AGO7, and DCL2 can act with partial redundancy with
381 their respective paralogs (Borges and Martienssen, 2015). Homologs of all core *Arabidopsis*
382 PTSG components including two *AGO2*, two *AGO7*, four *AGO10* and three *DCL2*-like genes
383 were identified in the cowpea genome. All of the core components required for *Arabidopsis*-
384 like PTGS were expressed during male gametogenesis except for *RDR6*, which was
385 undetectable or expressed at very low levels in all male cell-transcriptome types and at low
386 levels in the mature pollen-sperm cell sample. By contrast, moderate *RDR6* expression was
387 evident together with similar or higher expression of the PTSG components in the leaf
388 transcriptome (Fig. 6A and Supplemental Table 10 and 11). The typical *Arabidopsis*-like PTSG
389 pathway may not be active during cowpea male gametogenesis.
390
391 The *Arabidopsis* RdDM pathway results in the production of 24nt siRNAs and site-specific *de*
392 *novo* methylation at their target DNA sites by DNA methyltransferases MET1 and DRM2
393 (Borges and Martienssen, 2015). Genes required for RdDM including *AGO4*, *AGO5*, *DCL3*,
394 *RDR2*, *NRPD1* and *NRPE1* (encoding the largest subunits of POL IV and V respectively) were
395 detected at various stages during male gametogenesis. Transcript levels of *NRPD1*, *RDR2*
396 and *DCL3* were relatively low. However, highest transcript levels of DNA methyltransferase
397 *MET1*, *DRM2_1* and *DRM2_2* were evident during male meiosis, decreasing during the
398 mitotic events of gametogenesis (Fig. 6B and Supplemental Table 11). This suggests an
399 *Arabidopsis*-like RdDM pathway is likely to be functional during cowpea male
400 gametogenesis.

401

402 Other DNA methyltransferases including CMT2 and CMT3 DNA can maintain CHG/CHH and
403 CHG methylation, respectively, independently from the RdDM pathway in *Arabidopsis*.
404 Cowpea homologs of both genes were strongly expressed during male meiosis and mitosis
405 (Fig. 5B). Interestingly, high transcript levels from the DNA glycosylase *DME* that mediates
406 DNA demethylation by removing methyl-cytosine and replacing it with unmethylated
407 cytosine in *Arabidopsis* (Penterman et al., 2007) were found during early cowpea PMC
408 meiosis (Fig. 6B and Supplemental Table 13). Collectively, these data suggest multiple
409 pathways inducing dynamic DNA methylation changes may operate during cowpea male
410 gametogenesis.

411

412 Changes in chromatin histone composition are known to occur during pollen development
413 in *Arabidopsis*. A total of 44 cowpea histone genes belonging to the core histone families
414 H2A, H2B, H3 and H4 were identified in cowpea (Talbert et al., 2012); Fig. 6A and
415 Supplemental Table 12), and their expression profiled during male gametogenesis. A
416 prevalence of H3.3 histone transcript variants are evident in mature *Arabidopsis* pollen and
417 H3.1 variants were absent (Borg and Berger, 2015). Analysis of histone gene transcription
418 during cowpea male gametogenesis showed high levels of the core histone H3.3 transcripts
419 throughout male gametogenesis, including the mature pollen-sperm cell sample. H3.1_3
420 histone transcript levels were also detected during male gametogenesis but were
421 undetectable in the mature pollen-sperm cell sample, as was a range of other cowpea
422 histone transcripts (Fig. 6A). These data suggest conservation of transcriptional patterns of
423 H3.3 and 3.1 expression during pollen maturation in cowpea and *Arabidopsis*.

424

425 Epigenetic processes involving the Polycomb-group repressive complex 2 (PRC2), which
426 applies a repressive trimethylation mark on lysine 27 of histone H3 (H3K27me3) regulate a
427 number of events in the plant lifecycle. Proteins forming the PRC2 complex vary in relation
428 to these functional contexts (Fig. 6B). In *Arabidopsis*, the PRC2 VRN complex, containing
429 CLF/SWN, VRN2 and FIE proteins, functions during vegetative development and the floral
430 transition, whereas the EMF complex, containing FIE, MSI1, CLF/SWN and EMF2, functions
431 during inflorescence development and flower organogenesis. The PRC2 FIS complex,
432 containing MEA/SWN, FIS2, FIE and MSI1, functions to silence target genes during early seed
433 development and gametogenesis (Pien and Grossniklaus, 2007). Cowpea homologs of
434 *Arabidopsis FIE, MSI1, EMF2, VRN5, VIN3* and *EMF1* genes were co-expressed during male
435 gametogenesis. (Fig. 6C). High levels of a cowpea *SWINGER*-like (*SWN*-like) transcript were
436 observed during late pollen mother cell meiosis and microspore formation. The expression
437 patterns of the PRC2 complex-like genes during male gametogenesis in cowpea suggest
438 there is a potential for the formation and function of novel, possibly multiple PRC2
439 complexes resembling modified versions of the EMF and VRN PRC2 types during male
440 gametogenesis.
441
442 Jumonji-domain proteins (JMJ) function to demethylate histones, antagonizing the
443 establishment of histone methylation. *JMJ706_1*, *JMJ16* and *JMJ25_1* and *JMJ25_5*-like
444 genes, potentially encoding proteins which demethylate histone methylation marks, other
445 than H3K27 (Fig. 6D) were expressed at elevated levels during cowpea male gametogenesis
446 (Fig. 6D). In rice, JMJ706 regulates transcription factor expression required for spikelet
447 development, floral morphology and organ number (Sun and Zhou, 2008) *Arabidopsis* JMJ16

448 represses leaf senescence (Liu et al., 2019) and JMJ25 functions in poplar to remove
449 H3K9me2 marks and modulate anthocyanin biosynthesis (Fan et al., 2018).
450
451 **Gene expression during temporal events of cowpea female gametophyte formation**
452
453 Meiosis-related genes were expressed at a number of stages during female gametophyte
454 development as also observed during male gametogenesis. Transcript levels of meiosis
455 genes were evident at lower levels throughout female gametogenesis (Fig. 3C). Auxin
456 biosynthesis gene transcripts were detected from *YUCCA* and *TAR*-like genes during cowpea
457 megaspore mother cell meiosis (Fig. 4A). In contrast with male gametophyte development,
458 auxin biosynthesis gene transcripts were generally undetectable in developing cowpea
459 female gametophytes in most of the post-meiotic developmental stages. Exceptions were a
460 *TAR2_3*-like gene expressed at relatively low levels throughout the stages of female
461 gametogenesis, which was also expressed throughout male gametogenesis, during early
462 embryogenesis and in leaf (Fig. 4A). *YUCCA6, 8, 10* and *TAR4_2*-like genes were co-
463 expressed in the EC and CC with *TAR2_2* showing higher relative EC expression (Fig. 4A;
464 Supplemental Table 9).
465
466 In direct contrast to the subdued nature of auxin biosynthesis gene expression in developing
467 female gametophytes, a total of 47 genes annotated generally as "auxin-responsive" were
468 expressed with RPM counts over 10 in cell-types of the developing female gametophyte
469 (Fig. 4B and Supplemental Table 9). These genes included 15 *AUXIN RESPONSE FACTORS*
470 (*ARF*s and five *AUX-IAA* genes, five auxin transporters belong to the *LAX* and *BIG* gene
471 families, two polar auxin transport *PIN* homologs and three *SMALL AUXIN UP RNA* (SAUR)

472 which are induced in response to auxin (Fig. 4B and Supplemental Table 9). The auxin
473 induced *AIR12*-like gene was expressed at high levels in both the 4 nucleate and the mature
474 embryo sacs, which suggests that regulation of reactive oxygen species may be important if
475 the function of *Arabidopsis* AIR12 is conserved in cowpea.
476
477 The expression of gene components required for *Arabidopsis*-like micro-RNA-mediated
478 silencing was evident during female gametophyte development. Low levels of *DCL1*, *HYL* and
479 *HEN* were observed in the mature embryo sac. The relative expression of *DCL1* was
480 approximately five times higher in the EC than CC (Figure 5A and Supplemental Table 11).
481 These observations suggest that miRNA induced gene silencing is ongoing during the events
482 of meiosis and mitosis during female gametogenesis. Potentially, miRNA production may be
483 more active in the egg than the central cell in mature embryo sacs.
484
485 Examination of expression of homologs of genes involved in the *Arabidopsis* PTGS pathway
486 showed non-detectable *RDR6* expression as also observed during in male gametogenesis.
487 Thus either the typical PTGS pathway described for *Arabidopsis* is not active within male and
488 female cowpea reproductive cell types examined, or other cowpea-specific elements
489 substitute for generation of 21-24 nt siRNAs (Fig. 5A).
490
491 Expression of the RdDM pathway components during female gametogenesis suggested
492 functional gene silencing is active during meiosis and mitotic events. High expression levels
493 of *DME* were also observed in the post-meiotic megaspore tetrad and bi-nucleate mitotic
494 embryo sacs, suggesting methylation turnover is required for the initiation of the mitotic
495 embryo sac progression (Fig. 5B). Interestingly, expression of both *AGO4* and *AGO5* were

496 approximately two times and five times higher in the EC than in the CC, respectively. In
497 addition, *MET1* and *DRM2_1* were expressed at three-fold and 1.5-fold higher levels in the
498 EC than CC, respectively. This suggests relatively lower gene silencing activity via the RdDM
499 pathway in the CC than in the EC (Fig. 5B and Supplemental Table 11). Expression of
500 homologs of *CMT2* and *CMT3-B* which maintain methylation independently from RdDM
501 were approximately three times lower in egg than in central cell (Fig. 5B and Supplemental
502 Table 11). These results suggest a hypothesis that possibly *de novo* DNA methylation via the
503 RdDM pathway may be reduced in the cowpea CC compared to the EC, while maintenance
504 of CHG and CHH methylation may be higher in the cowpea CC than the EC. DNA methylation
505 turnover in the EC and CC may be mediated by *DME* and ROS as indicated by moderate
506 levels of expression in these cell-types (Fig. 5B).
507
508 Most core histones including *H3.3-1* were expressed at moderate levels during female
509 development in cowpea. (Fig. 6A and Supplemental Table 14). The MMC showed higher
510 relative levels of histone *H3.3_1*, *H4_1, 2*, and *3.1_1* transcripts. *Histone3.3* variants were
511 expressed throughout gametogenic development, as were a number of *H3.1* variants which
512 contrasts with the trend observed in male gametogenesis (Fig.6A). High transcript levels of
513 the JMJ25-like gene were evident at MMC meiosis, together with moderate levels of the
514 JMJ706 H3K9 demethylase as seen in late pollen mother cell meiosis, suggesting a possible
515 requirement for H3K9 demethylation in both male and female cowpea meiosis. Expression
516 of the JMJ histone demethylase JMJ30, which removes H3K27me2/3 deposited by PRC2
517 complexes was higher in the female gametophyte than the male (except for the MP-SC
518 sample; Fig. 6D; Supplemental Table 14).
519

In *Arabidopsis*, the PRC2 FIS complex, containing MEA/SWN, FIS2, FIE and MSI1, functions to silence target genes during embryo sac maturation and early seed development (Mozgova and Hennig, 2015, Grossniklaus and Paro, 2014). Dynamic expression patterns of a number of PRC2-like gene homologs were expressed during cowpea female gametogenesis, including *FIE*, *MSI1*, *EMF1*, *EMF2*, *EMF2*-like, *CLF* and *VRN5* (Fig. 6C). In the mature embryo sac, egg and central cell samples, *FIE*, *MSI1*, *EMF2_2*, *EMF2*-like, and *VRN5_2* were all co-expressed. High levels of *FIE*, *EMF2*-like, and *VRN5_ 2* were evident in the central cell (Fig. 6C). Given the multimeric protein composition of PRC2 complexes, it is not possible to predict the composition of one or more potential complexes that might be functioning during cowpea female gametogenesis from these transcriptional analyses.

Cell cycle arrest in egg and central cells

Cell cycle genes are relatively well conserved across plant species (Wang et al., 2004, Scofield et al., 2014). Analyses of the expression of cell cycle genes known to block and/or promote passage through various phases of the cell cycle in isolated cell types has been used to predict the stage of cell cycle arrest (Juranic et al., 2018, Sornay et al., 2015, Sukawa and Okamoto, 2018, Velappan et al., 2017, Komaki and Sugimoto, 2012). A core set of cell cycle genes from *Arabidopsis* was used to identify 141 non-redundant cowpea genes encoding proteins with various roles in cell cycle regulation, including 46 cyclins (CYC), 12 cyclin-dependent kinases (CDKs) and 5 CDK inhibitors (interactor/inhibitor of cyclin-dependent kinases/Kip-related proteins; KRP/ICKs) in addition to other key regulators (Supplemental Table 15 and 16). The expression of these in the central cell and egg cell

542 transcriptomes was used to predict the stage of arrest in both cell-types in mature cowpea
543 female gametophytes (Fig. 7).
544
545 The transition from G1 to S phase requires activity of CDKA/CYCD complexes to
546 phosphorylate, and inactivate RBR, thereby enabling E2F transcription factors to drive S-
547 phase gene expression (e.g. genes such as *PCNA* and *MCM2-7*; (Dante et al., 2014).
548 Functional activity of the CDKA/CYCD complex at the G1/S transition is also inhibited by
549 KRP/ICKs, which act on additional CDK/CYC complexes to block transition from G2 to M
550 (Dante et al., 2014). The protein kinase, Wee1 can contribute to a block in cell-cycle
551 progression at the G2/M transition (De Schutter et al., 2007). The MYB3R family members,
552 MYB3R1 and MYB3R4 transcriptionally activate many G2/M promoting genes (Haga et al.,
553 2011). MYB3R3 and MYB3R5 negatively regulate transcription of the same genes (Kobayashi
554 et al., 2015). However, MYB3R1 can also negatively regulate transcription, redundantly with
555 MYB3R3 and MYB3R5 at G2/M (Kobayashi et al., 2015).
556
557 The egg cell appeared to be arrested in G1/S because expression of RBR and three KRP-like
558 genes *KRP7/ICK5_1*, *KRP3/ICK6_1* and *KRP3/ICK6_2* was moderate to high in the EC.
559 Expression of the *CYCD*s (*CYCD2*, *CYCD3*, *CYCD5* and *CYCD6*), indicative of G1 phase, was low
560 to moderate in the EC while expression of S-Phase genes was moderate to high (Fig. 4,
561 Supplemental Table 16). The high expression of two repressive *MYB3R5* homologs
562 (*MYB3R5_3* and *MYB3R5_4*) and three *Wee1* homologs (*Wee1_1*, *Wee1_2* and *Wee1_3*) in
563 the EC (Fig. 7, Supplemental Table 16) suggests that it is unlikely the EC can progress
564 through the G2/M transition (Kobayashi et al., 2015).
565

566 The central cell appeared to have progressed past S phase and appeared to be arrested in
567 G2/M because *RBR1* and *KRP7*/*ICK5_1* expression were strongly reduced compared to that
568 in the EC, as was expression of all S phase-related genes (Fig. 5, Supplemental Table 16). The
569 expression of three *CYCB*-like homologs promoting the G2/M transition, (*CYCB2;3_1*,
570 *CYCB2;3_2* and *CYCB1;2.1_2*) showed high expression in CC at almost three times that
571 observed in the egg cell (Fig. 5, Supplemental Table 16). The CC showed only moderate
572 expression of two G2/M promoting *MYB3R1* homologs, expression of repressive *Wee1_1*
573 and *Wee1_2* was moderate and *MYB3R4* and *MYB3R5* expression was low to undetectable
574 (Fig. 5, Supplemental Table 16). Taken together, these data indicate the cowpea CC is
575 preparing to enter M phase.
576
577 **Post-fertilization gene expression in cowpea**
578
579 The GO terms characterizing the early post-fertilization embryo transcriptome comprised of
580 elongating egg cells, zygotes and early embryos, provided signatures of growth with
581 microtubule movement, cell proliferation, transcription, translation carbohydrate processes,
582 and cell wall biogenesis (Fig. 3A). Meiosis transcript expression was restricted to homologs
583 of *MSH4*, *PRD1*, *OSD1* and *SMG7* (Fig. 3C). A range of auxin biosynthesis-like genes were
584 expressed including *YUCCA*-likes, *2*,*3*,*4*, *6*, *8* and *10* and *TAR10*-like (Fig. 4A). By contrast, a
585 lower repertoire of auxin-responsive type gene expression was observed relative to that
586 seen during male and particularly female gametophyte formation (Fig. 4B). Evidence for
587 extensive microRNA-induced silencing was low given the low levels of *HEN* and *DCL1*.
588 Activity of an *Arabidopsis*-like PTGS pathway was unlikely with many components
589 undetectable (Fig. 5A), and significant RdDM activity at the cell-type stages collected was

590 also doubtful. Expression of other DNA methylation components was evident as was
591 expression of the DNA demethylase *DME* (Fig. 5B). A repertoire of histones genes were
592 expressed and expression of a number of PRC2-like genes suppressed. High levels of *JMJ25*-
593 like gene expression were noticeable suggesting H3K9 demethylation may be supporting
594 early cowpea embryogenesis (Fig. 6D).

595 **Discussion**

596 **Cowpea reproductive cell-type transcriptomes: a legume resource**

597

598 The generated cowpea transcriptomes spanning the temporal sequence of events during
599 male and female gametophyte and early seed development enabled detection of enriched,
600 specifically expressed genes including cell-type specific genes expressed at low levels.
601 Verification levels of 71% of cell-type specific expression by qRT-PCR and spatial
602 confirmation *in situ* hybridization confirmed the utility of these transcriptomes for further
603 dissection of regulatory networks in cowpea and syntenic legumes. Comparative analyses of
604 cowpea cell-type specific genes and those specifically expressed in *Arabidopsis*, led to the
605 identification of *Arabidopsis*-derived promoters directing gene expression to meiotic cells,
606 the egg and central cells and early embryos of cowpea. This supports the conservation of
607 some regulatory transcriptional networks during reprodutive cell differentiation in both
608 cowpea and *Arabidopsis*.

609

610 The cowpea meiosis genes identified show strong conservation with those found in other
611 angiosperms. Cowpea meiosis genes were, however, found to be expressed at moderate
612 levels in non-meiotic cell-types. *Arabidopsis* tissue RNAseq experiments have also found

613 that meiosis genes are present in many tissues throughout development (Klepikova et al.,
614 2016). This is consistent with their roles in DNA repair, cell-cycle control and recombination,
615 and highlights the likely role of cell-specific protein-protein interactions in determining their
616 molecular function in either meiosis or mitosis (Cromer et al., 2012).
617
618 With respect to the involvement of epigenetic pathways during cowpea reproductive
619 development, genes encoding cowpea AGO proteins were identified, and transcriptome
620 analysis suggests an *Arabidopsis*-like RdDM pathway is likely to regulate a number of
621 reproductive stages. *AGO5*, *AGO4* and *AGO6*-like are expressed throughout female
622 gametogenesis. Previous work has suggested that *Arabidopsis AGO5* is expressed in
623 sporophytic tissue and plays an important role in defining the MMC prior to meiosis, but is
624 absent from female gametophyte tissue during subsequent development (Tucker et al.,
625 2012). The roles of RdDM in female gametophyte development may differ between
626 *Arabidopsis* and cowpea, and this can be functionally tested.
627
628 By contrast, an *Arabidopsis*-like PTGS pathway does not appear to be functional in the
629 stages analyzed because RDR6 expression, while detectable in leaf, was not expressed in
630 reproductive cell-types. An alternative component may substitute for RDR6 in cowpea
631 reproductive cells. The cowpea cell-type transcriptomes also suggested potential for PRC2-
632 like complex formation and function during male and female gametophyte formation. The
633 data revealed the possibility for a number of novel combinations of proteins in such
634 potential cowpea-PRC2 multimeric complexes. The identified gene candidates could be
635 tested in protein interaction studies, and mutagenic approaches to confirm complex
636 components and their functional relevance. Additional insights into pathways evident during

637 cowpea reproductive development which have been uncovered from *in silico* analyses are
638 discussed further below.
639
640 **Plant hormone pathways involved in cowpea reproductive development and patterning**
641
642 Plant hormones contribute significantly to plant differentiation and growth. In both the
643 megaspore mother cell and late pollen mother cells, GO terms for "abscisic acid (ABA)
644 signalling pathway" and response to abscisic acid were enriched. Underpinning genes were
645 predicted to encode homologs of calcium-dependent protein kinases involved in ABA signal
646 transduction that influence panicle development and seed formation in rice (Ray et al.,
647 2007). Homologues of genes involved in the biosynthesis of brassinosteroids, a HERK
648 receptor-like kinase and a SCARECROW-like transcription factor, involved in perception and
649 positive regulation of brassinosteroid-mediated gene expression, were expressed during
650 female embryo sac mitosis. In addition, homologs of genes functioning in reproductive
651 development in other species, and involved in synthesis and perception of jasmonic acid and
652 cytokinin were upregulated in mature embryo sacs (Li et al., 2004, Bartrina et al., 2011, Kim
653 et al., 2005). Functional roles of these genes in cowpea remain to be determined.
654
655 Auxin biosynthesis and auxin-responsive genes were upregulated during early cowpea
656 pollen development, reflecting the functional requirement for auxin in early *Arabidopsis*
657 pollen development (Yao et al., 2018). Auxin biosynthesis is also considered important
658 during *Arabidopsis* female gametophyte development. For example, the auxin biosynthesis
659 genes *YUCCA1* and *YUCCA2* are considered to be required early for cell specification. Later
660 expression of *YUCC8*, *TAA1* and *TAR2* biosynthesis genes are required for nuclear

661 proliferation, vacuole formation and embryo sac growth (Panoli et al., 2015). Studies have
662 suggested an auxin gradient serves as the morphogen driving female gametophyte cell
663 specification in *Arabidopsis* (Pagnussat et al., 2009). However, auxin activity has not been
664 experimentally determined in the developing *Arabidopsis,* maize and *Hieracium pilosella*
665 female gametophytes during mitotic divisions (Lituiev et al., 2013).
666
667 While *YUCCA* and *TAR*-like auxin biosynthesis genes were expressed in the cowpea female
668 megaspore mother cell, the expression of auxin biosynthesis genes was barely detectable in
669 subsequent stages of megagametogenesis except for low levels of *TAR2*. Expression of
670 *YUCCA6*, *8* and *10* homologs, and *TAR2* and *TAR4* homologs was detected at low levels in
671 the egg and central cell of the mature embryo sac. The auxin response machinery including
672 multiple *ARF* transcription factors, *AUX-IAA* genes, *SAUR* genes and auxin transporters was
673 detected at moderate to high levels. Highest expression levels were evident in the egg cell
674 and central cell. In the presence of low levels of auxin, AUX-IAA proteins interact with the
675 ARF transcription factors and inhibit transcription of auxin responsive genes. At higher auxin
676 levels, AUX-IAA proteins are degraded by the ubiquitination pathway, freeing the ARF
677 transcription factors to promote expression of their target genes (Wang and Estelle, 2014).
678
679 Given that expression of auxin biosynthesis genes was very low in the developing cowpea
680 female gametophytes, this may indicate that some auxin-related processes are suppressed.
681 The contrasting pattern of very low levels of auxin biosynthesis gene expression and higher
682 relative abundance of auxin responsive genes and transporters suggests that if auxin is
683 involved in cowpea female gametophyte patterning it may be transported in from the
684 sporophytic tissues post-meiosis. Experiments using auxin sensors in transgenic cowpea may

685 resolve this possibility. Alternatively, auxin may have effects in cowpea sporophytic tissue
686 that indirectly affect cell fate decisions in the female gametophyte as has been suggested
687 for *Arabidopsis* and maize (Lituiev et al., 2013).
688
689 **Cell cycle arrest in male and female cowpea gametophytes: involvement of epigenetic**
690 **regulation**
691 Unlike most other eukaryotes, where the gametes remain in the G1 cell cycle phase through
692 nuclear fusion at fertilization (karyogamy), higher plants form gametes that undergo
693 karyogamy in G1, S or G2 phases of the cell cycle (Friedman, 1999). We observed that
694 cowpea pollen is predominantly bi-cellular, containing a vegetative and a generative cell at
695 maturity, as approximately 10% of pollen grains contained a vegetative cell and two sperm
696 cells. Therefore, the events of pollen mitosis II in cowpea continue after pollen-tube
697 germination. *Arabidopsis* pollen grains are tri-cellular and sperm cells progress through S-
698 phase after pollen germination to arrive at G2 immediately prior to fertilization (Friedman,
699 1999).
700
701 Although the cell cycle stage of cowpea sperm cells at fertilization remain to be determined,
702 similarities in histone transcription were observed between *Arabidopsis* and cowpea during
703 pollen maturation. Histone *H3.3* and *H3.1* transcripts were detected during cowpea male
704 gametophyte formation, but histone *H3.1* transcripts were not detected in the mature
705 cowpea pollen-enriched sperm cell sample, as is also observed in *Arabidopsis*. H3.3 variants
706 correlate with gene expression in *Arabidopsis*, while H3.1 variants are incorporated during
707 the S-phase of the cell cycle (Borg and Berger, 2015), and references therein). In rice, EMF2
708 function is essential for pollen development, and it is thought to interact with a rice MSI1

709 homolog, PTC1 (Deng et al., 2017). Genes encoding homologs of a number of these PRC2
710 components were also expressed in cowpea pollen development and may have comparable
711 roles.
712
713 The central cell and egg cell are arrested at different stages of the cell-cycle prior to
714 fertilization. Studies in maize, rice, barley and *Arabidopsis* suggest that the egg is arrested at
715 G1 (Chen et al., 2017, Mogensen and Holm, 1995, Sukawa and Okamoto, 2018), while, in
716 *Arabidopsis,* it has been proposed that the central cell is most likely to be at G2 (Berger et
717 al., 2008). Analysis of cell cycle gene expression in cowpea egg and central cells indicated
718 their likely arrest in G1/S and G2/M cell cycle phases, respectively, consistent with that for
719 *Arabidopsis.*
720
721 Epigenetic pathways involving RdDM and DNA methylation repress transposon activity and
722 regulate female gametophyte arrest. DNA methylation is very low in the central cell and
723 reduced in the egg cell (Kawashima and Berger, 2014). RdDM and DNA methylation are
724 decreased in the central cell, and this allows expression of transposons, which are normally
725 repressed. Subsequent production of siRNAs that then direct methylation within the egg
726 cell, prevent transposon activation (Ibarra et al., 2012). In cowpea, expression of *AGO4*,
727 *AGO5* and *MET1* homologs was several times lower in the central cell than in the EC,
728 suggesting that *de novo* RdDM may also be less active in the central cell. Furthermore, the
729 miRNA pathway is likely more active in the cowpea egg cell than in the central cell as the key
730 components, *AGO1* and *DCL1* are expressed around five times higher in the egg cell. This
731 corresponds with observations of Wuest et al. (2010), who reported high egg cell expression
732 levels of *DCL1* and *AGO1* in *Arabidopsis.*

733

734 The transcriptome analyses also suggested that one or more novel PRC2-like complexes may
735 function to repress female gametophyte initiation in the absence of fertilization via histone
736 methylation. The conservation of a post-fertilization role of auxin in facilitating embryo
737 patterning in cowpea is supported by the observation of increased transcription of auxin
738 biosynthesis genes in the embryo as found in other species (Hands et al., 2016).

739

740 **Conclusions**

741 In this study, we have isolated and analysed cell-specific transcriptomes spanning the events
742 of male and female gametogenesis and early seed formation in cowpea. Cell-specific genes
743 were identified and validated using a combination of techniques including qRT-PCR and *in*
744 *situ* hybridization. The transcriptomes have identified gene expression pathways in common
745 with reproduction in other angiosperms, in addition to novel differences that can be
746 functionally examined. These cowpea reproductive cell-type transcriptomes provide a useful
747 resource for the further isolation of cell-type specific promoters, and uncovering
748 informative pathways which may aid in improving reproductive resilience and yield in
749 cowpea and related legumes.

750 **Materials and Methods**

751 **Plant material, tissue collection and generation of RNA sequences**

752 Cowpea plants (*Vigna unguiculata* IT-86D-1010) were grown in the glasshouse under
753 previously described conditions (Salinas-Gamboa et al., 2016). To collect RNA samples,
754 tissues at appropriate developmental stages were fixed and processed for LCM according to
755 previously published protocols (Okada et al., 2013). To collect sperm cells, anthers and

stigmas were collected from flowers at anthesis and subjected to osmotic shock in Brewbaker and Kwack medium (Brewbaker and Kwack, 1963), pH 6.5, supplemented with 12.5% (w/v) sucrose in 15 ml centrifuge tubes. The homogenate was centrifuged at 130 rpm, for 30 minutes at room temperature, then filtered through 150 µm and then 30 µm CellTrics nylon sieves (Partec GmbH) and collected in 2 ml microfuge tubes. The homogenate was centrifuged at maximum speed for 2 minutes to pellet cells, and 50 µl was layered on 0.5ml of 10% Percoll in 2ml microfuge tubes that were centrifuged at 900xg for 2 minutes. 1.5 ml of a solution of 0.52 M (10%) mannitol, 10 mM MOPS buffer (pH 7.5) was added, and the tubes were centrifuged for 2 minutes at maximum speed. 20µl of the resulting pellet was added to 30ul of ARCTURUS PicoPure RNA isolation buffer and snap frozen in liquid nitrogen before storing at -80C. Total RNA was extracted from the LCM samples and sperm cell enriched samples using the ARCTURUS® PicoPure® RNA Isolation Kit (Applied Biosystems®) according to the manufacturer's protocol. RNA was subjected to two rounds of amplification (three rounds for fTET, ES2n and ES4n) using the MessageAmp II RNA amplification kit (Ambion). Total RNA was extracted from leaf as described (Spriggs et al., 2018).

Sequencing and read alignment

Illumina sequencing libraries were prepared from the RNA samples by the Australian Genome Research Facility (AGRF) and run on the Illumina HiSeq2500 sequencing platform multiplexed in 3 lanes. At least 36 million reads were produced per sample (approximately 1.6 billion reads, total) of which ~86% could be uniquely aligned to the IT86D-1010 genome (Spriggs et al., 2018) using the BioKanga software package (Supplemental Table 1, Supplemental Data 8). A total of 74,839 genes were predicted in the cowpea IT86D-1010

genome (Spriggs et al., 2018) using Augustus v 3.1.0 (Stanke and Waack, 2003) and *Arabidopsis thaliana* (TAIR 10) as the gene training set. As no correlation between gene length and number of reads aligned was observed (Pearson´s correlation coefficient = -0.010), the Reads-Per-Million (RPM) normalization factor was used in all cases reporting normalized read counts. The RPM normalized counts between replicates of a cell-type sample were strongly positively correlated, with a Pearson's correlation coefficient (PCC) over 0.8 for most samples. Exceptions were replicates in the megaspore mother cell (MMC; PCC = 0.72), two-nucleate female gametophyte (ES2n; PCC= 0.766) and the pollen microspore (MIC; PCC = 0.62; Supplemental Fig. 1).

R versions and rsgcc analyses

Analyses made using R software packages used R Studio version 1.0.143, with R version 3.4.3 running under Windows 10. The rsgcc software of Ma and Wang (2012) was used as described by Zhan et al. (2015). The mean RPM normalized counts from each cell-type was used together with the getsgene() function of the rsgcc R package (rsgcc version 1.0.6) with the following parameters "getsgene(data, Log = FALSE, tsThreshold = 0.50, MeanOrMax = "Max")".

Gene Ontology annotations

Annotations were made by aligning the predicted IT86D-1010 coding sequences (Supplemental Data 9) against the NCBI nr protein database (version December 23rd 2017) using the DIAMOND aligner (Buchfink et al., 2015), version 0.9.13 returning at most ten alignments with a maximum e-value of 1e-5. The generated XML file was supplied to Blast2GO (version 5.0.13 running on windows 10 with Java version 1.0.8 152), which was run

804 with default parameters, to assign Gene Ontology (GO) annotations (Ashburner et al., 2000,
805 The Gene Ontology, 2017) to each predicted gene. This approach assigned putative
806 functional annotations to 54,223 predicted genes, with 39,653 predicted genes assigned GO
807 terms (Supplemental Data 1).
808
809 **Filtering to identify cell-specific genes in the egg cell, central cell and sperm cell**
810 **transcriptomes**
811 Genes specifically expressed in central cell, egg cell and sperm were selected using the filter
812 function in Microsoft Excel to choose genes with a mean RPM at least five times higher in
813 the cell-type of interest than any other cell-type (see full criteria in Supplemental Table 2).
814 No filter was applied to other cell-types in the female gametophyte when selecting egg cell
815 and central cell genes where the contrast between those two cells was the key criteria.
816
817 **Differential expression analysis**
818 Differential expression analysis was carried out using the DESeq2 (version 1.18.1) software
819 package in R (Love et al., 2014). Analyses were carried out as described except that
820 differentially expressed genes in each cell-type were identified using the contrast argument
821 of the results function with parameters set to contrast the expression of each gene in one
822 cell-type with the average expression of all other cell-types "results(dds, contrast =
823 list(c(cell_X), c(all_other_cells)), listValues = c(1, -1/13), alpha = .05)". Genes with adjusted p
824 value < 0.05 and log2 fold change > 2 were selected as significant (Supplemental Data 5).
825
826 **Principal Component Analysis**

827 Principal component analysis was carried out on each replicate of our developed
828 transcriptomes using the base R prcomp() function on read counts transformed by the
829 variance stabilising transformation, vsd(), function of DESeq2. Principal components were
830 plotted in 3D using the plot3d() function of the rgl package. Colours suitable for all vision
831 types were chosen from the colour alphabet previously described (Green-Armytage, 2010).
832 Plots were exported as .svg files and figures were assembled in Adobe Illustrator.
833
834 **Comparisons between cowpea and Arabidopsis female gametophyte LCM data sets**
835 The best *Arabidopsis* homolog for each predicted cowpea gene was identified by using the
836 DIAMOND aligner (Buchfink et al., 2015) (version 0.9.13) to align cowpea genes against the
837 TAIR 10 gene database, and selecting the best match for each cowpea gene (Supplemental
838 Data 7). *Arabidopsis* gene sets from the MMC (Schmidt et al., 2011), ovule nucellus, early
839 mitotic female gametophytes (Tucker et al., 2012) and the egg and central cell (Wuest et al.,
840 2010, Steffen et al., 2007) were compared with the *Arabidopsis* annotations of each cowpea
841 gene in the differentially expressed genes (log2 fold-change >2) in corresponding cell-types
842 from the cowpea dataset.
843
844 **Identification of core meiosis, auxin biosynthesis, auxin-responsive genes and cowpea cell-**
845 **cycle genes**
846 A set of 18 core cowpea meiosis genes were identified by BlastP search of key genes in the
847 literature (Supplemental Table 7 and references therein) against the amino acid sequence of
848 the cowpea IT86D-1010 predicted genes. In each case the best match based on bit-score
849 was chosen for further analysis. To identify cell-cycle related cowpea genes, the amino acid
850 sequences of a set of cell-cycle genes from *Arabidopsis* (Juranic et al., 2018) were used in

BlastP searches against the predicted cowpea protein sequences. BlastP results with an e value < 1e-20 were chosen, and the annotation of cowpea sequences matching multiple *Arabidopsis* genes was chosen based on the highest bit score. The *KRP* gene family and *cdc*25 homologs were selected with an e value < 1e-10. Where multiple cowpea genes matched a single *Arabidopsis* gene, these were notated with an underscore and number after the gene name starting with 1 for the best match and increasing (e.g. VuGene_1). Auxin-related genes were identified in the laser captured cell-type transcriptomes, based on their GO annotations (Supplemental Table 9).

Identification of cowpea RNA silencing, RdDM and histone genes

A total of 37 key genes in RNA silencing and RdDM pathways were identified by searching the annotations produced by the Blast2GO software for genes described in key literature (Supplemental Table 10). Fragments not encoding full length protein homologs were not included in further analysis.

A total of 49 putative histone encoding genes and 20 JMJ homologs were identified in annotations produced by Blast2GO as described above. The predicted histone variant encoded by each gene was assigned based on annotations, and on homology of the predicted protein to *Arabidopsis* histone amino acid sequence (Supplemental Fig. 7).

Phylogenetic tree construction

Phylogenetic trees were made using Geneious version 10.2 (Biomatters, https://www.geneious.com). Trees were built using the following parameters: ClustalW multiple-sequence alignment with BLOSUM cost matrix, Gap open cost 10, Gap extend cost

874 0.1, Jukes-Cantor Neighbour-Joining consensus tree, no outgroup, Bootstrap resampling
875 with 1000 replicates, 50% support threshold.
876
877 **Validation by qPCR**
878 Whole tissues were collected from the following tissues, emerging leaves, developing stem,
879 petiole, shoot apical meristems and roots (Supplemental Table 3), frozen in liquid nitrogen
880 and RNA was extracted with a QIAGEN RNeasy Plant mini kit according to the
881 manufacturer's protocol, including on-column DNAse treatment. cDNA was synthesised
882 using 1ug of RNA with the SuperScript™ III First-Strand Synthesis System (Thermo Fisher
883 Scientific). Central cell and sperm genes were selected for testing by qPCR and *in situ*
884 hybridisation based on specificity in expression and putative function of the predicted
885 genes. Egg cell genes were chosen for testing based on the specificity of their expression
886 and homology to *Arabidopsis* genes known to be specifically expressed in egg cell. Genes in
887 other cell-types tested were selected based on their specificity score in the rsgcc analysis
888 and on our ability to design primer pairs (Supplemental Table 17) that specifically amplified
889 the predicted region, including intron structures, from genomic and cDNA. qRT-PCR was
890 carried out on a Roche Light Cycler ® 480 thermal cycler using SYBR Green I master mix
891 according to the manufacturer's protocols. Quantification was done using LinRegPCR
892 software as described (Ruijter et al., 2009, Ramakers et al., 2003).
893
894 **In situ hybridization.**
895 ISH was performed as previously described (Jackson, 1992) with some modifications for
896 improved resolution in reproductive organs of cowpea. For ISH performed on sectioned
897 specimens, mature unpollinated ovules were fixed in 4% paraformaldehyde and embedded

898 in Paraplast. Sections at 12 µg thickness were attached to ProbeOnPlus slides (Fisher
899 Biotech) and processed as previously described (Jackson, 1992). For whole-mount ISH,
900 developing ovule primordia, unpollinated mature ovules, and mature anthers were fixed in
901 paraformaldehyde (4% paraformaldehyde, 2% Triton, and 1× PBS in diethylpyrocarbonate
902 DEPC-treated water) for 2 h at room temperature with gentle agitation, washed three times
903 in 1× PBS-DEPC water, and embedded in 15% acrylamide:bisacrylamide (29:1) using pre-
904 charged slides (Fisher Probe-On) treated with poly-l-Lys as described (Bass et al., 1997).
905 Fixed pollen grains were stripped from the anthers before embedding, and incubated with
906 an enzymatic solution containing 1% driselase, 0.5% cellulose, and 1% pectolyase, for 30
907 minutes (min) in a humid chamber at 37ºC. All samples were subsequently incubated with
908 0.2M HCl solution for 30 min at room temperature (RT) and in 1ug/ul proteinase K for 30
909 min at 37ºC, before being processed as previously described (García-Aguilar et al., 2005).
910 Slides containing paraffin sections were mounted on Cytoseal, whereas slides containing
911 whole specimens were mounted in either 50% (ovules) or 20% (pollen grains) glycerol, and
912 analyzed with a Leica DMRB microscope under Nomarski illumination.
913
914 **Plasmid construction and cowpea transformation**
915 Gateway entry vectors containing cell-type specific promoter elements together with genes
916 encoding fluorescent proteins were gifts from Shai Lawit and Marc Albertsen (Lawit et al.,
917 2013) as follows: *AtDD1*$_{pro}$*:ZsYellow1*, *AtDD9*$_{pro}$*:DsRed-Express*, *AtDD25*$_{pro}$*:DsRed-Express*,
918 *AtDD31*$_{pro}$*:AcGFP1*, *AtDD45*$_{pro}$*:DsRed-Express*, *AtDD65*$_{pro}$*:AmCyan1*, *AtLat52*$_{pro}$*:AcGFP1*,
919 *AtRKD2*$_{pro}$*:DsRed-Express*. The promoter element of *AtEC1.1* was amplified from *Arabidopsis*
920 Col-0 DNA by PCR with primers including adapter elements, and cloned into gateway entry
921 vectors containing AmCyan1. The *AtDUO1* promoter was synthesized and cloned into pMK-

RQ by GeneArt (Thermo Fisher Scientific) with SfiI and BglII sites introduced for subsequent cloning into gateway entry vector containing AcGFP1.

A gateway-compatible binary vector pOREOSAr4r3 was created by insertion of a Gateway recombinational cassette amplified from pDESTr4r3 (Invitrogen) into ClaI and KpnI sites of pOREOSA vector backbone, which was a gift from Thomas J. Higgins, CSIRO. Reporter entry clones were introduced into the pOREOSAgw expression vector via multisite Gateway recombination. Final constructs contained either triple or quadruple fluorescent labels (Supplemental Table 20). AtKNU:YFP:3'KNU cassette was previously described (Tucker et al., 2012) and was inserted into the pOREOSA via HindIII digestion. Gateway cloning reactions were performed with LR Clonase II Enzyme mix (ThermoFisher Scientific). All plasmid vectors were verified by sequencing and final constructs electroporated into *Agrobacterium tumefaciens* strain AGL1 for use in cowpea stable transformation (see below). Details of the primer sequences and constructs transformed into cowpea are described in Supplemental Tables 19 and 20. Cowpea transformation was carried out using *Agrobacterium*-mediated transformation of cotyledonary nodes (Popelka et al., 2006). Transformed explants were first selected on a medium containing 100 mg/L kanamycin and then on 20 mg/L geneticin (G-418) for up to 3-6 months. Shoots developing healthy roots were transferred into 90mm small pots containing sterilized soil mixture (Van Schaik's Bio-Gro Pty Ltd, Australia), acclimatized in the growth room at 22°C with 16h photoperiod for up to 4 weeks, and then transferred to the glasshouse in larger 4.5L pots. PCR was performed to confirm the presence of the *nptII* and reporter genes with the primers listed in Supplemental Table 19. The number of independent cowpea transgenic lines per construct varied from three to 15.

945

946 **Fluorescent microscopy and clearing procedures**

947 Samples were examined using a Zeiss fluorescence microscope (Axio Imager M2; Carl Zeiss)
948 with an HXP 120 light source. Digital images were captured using an AxioCam HRc camera
949 and ZEN 2.6 software (Carl Zeiss). Signals from dsRED-Express were observed with the Zeiss
950 filter set 43, AcGFP1 signals were observed with the Zeiss filter set 13, AmCyan1 signals
951 were observed with Zeiss filter set 47, while YFP and ZsYellow1 signals were observed with
952 Zeiss filter set 46. The exposure time was adjusted to as appropriate for each sample.
953 Images were processed in ZEN2.6 software and assembled in Adobe Photoshop. The
954 method previously described in (Salinas-Gamboa et al., 2016) was used when tissue clearing
955 was required. For light microscopy, the Zeiss Axioskop 2 microscope equipped with
956 Nomarski optics, Spot Flex colour camera and Spot 5.1 software was used to capture images
957 (Diagnostic Instruments, Inc).

958

959 **Generation of transgenic *Arabidopsis* with cowpea promoter constructs**

960 The regulatory region of eleven cowpea genes was transcriptionally fused to the *uidA* (*GUS*)
961 reporter gene by amplifying a fragment corresponding to either the complete intergenic
962 region (*VuNB-RCpro; VuSDR1pro*) or an arbitrary fragment (*VuBAS1pro; VuGULL06pro;*
963 *VuRKD1pro; VuEC1.1pro; VuGIM2pro; VuXTH6pro; VuXTH32pro; VuAt3g09950pro; VuKNU-*
964 *L1pro*) located upstream of its coding sequence but excluding the 5′ untranslated region
965 (see Suppl Table 21 for primers). Amplicons were cloned into pCR8 TOPO TA (Invitrogen)
966 and used as donors in LR recombination (LR Clonase II; Invitrogen) with pMDC162 (Curtis
967 and Grossniklaus, 2003), producing a binary vector that contains the *uidA* reporter gene.

968 Transgenic Col-0 plants were obtained by floral dipping as previously described (Clough and
969 Bent, 1998). At least 15 T1 individuals were obtained and analyzed to quantify the
970 frequency of GUS expression at different stages of male and female reproductive
971 development. GUS staining assays for stages before fertilization were conducted as
972 described (Vielle-Calzada et al., 2000).
973

974 **Accession numbers**

975 **Large datasets**

976 .bam files of sequences from
977 TO BE CONFIRMED
978
979 Fasta.gz archives of raw reads for MMC, EM and Sp
980

981 **Supplemental Material**

982 **Supplemental Tables**

983 **Supplemental Table 1. Align stats**

984 Number and proportion of Illumina reads aligned against the IT86D genome for each sample

985 **Supplemental Table 2. Filtering**

986 Criteria and results of selecting genes based on filtering in Excel

987 **Supplemental Table 3. *Arabidopsis* Reproductive genes and promoters**

988 Summary of *Arabidopsis* reproductive cell-specific gene expression of their Cowpea

989 homologs in cowpea and activity of their promoters driving transgenes in *Arabidopsis*

990 **Supplemental Table 4. qPCR**

991 Table of tissues and results of qRT-PCR validation of cell-specific gene expression

992 **Supplemental Table 5. CS_DE_gene_overlap**

993 Table summarising the number of common genes between cell-specific and differentially

994 expressed datasets.

995 **Supplemental Table 6. Compare datasets**

996 Comparison of published cell-specific datasets with our transcriptomes

997 **Supplemental Table 7. Meiosis genes**

998 Names and references for the cowpea homologs of genes involved in meiosis

999 **Supplemental Table 8. Meiosis RPM**

1000 Expression of meiosis genes as RPM counts

1001 **Supplemental Table 9. Auxin genes**

1002 Expression of annotated auxin related genes as RPM counts

1003 **Supplemental Table 10. RNAi, RdDM refs**

Names, functions and references for the cowpea homologs of genes involved in RNA silencing and RdDM

Supplemental Table 11. RNAi, RdDM RPM counts

Expression of RNAi and RdDM genes as RPM counts

Supplemental Table 12. Histone RPM counts

Expression of histone genes as RPM counts

Supplemental Table 13. PRC RPM counts

Expression of PRC genes as RPM counts

Supplemental Table 14. JMJ RPM counts

Expression of JMJ genes as RPM counts

Supplemental Table 15. Cell-cycle genes

Names and references for the cowpea homologs of genes involved in cell-cycle progression

Supplemental Table 16. Cell-cycle RPM

Expression of cell-cycle genes as RPM counts

Supplemental Table 17. Oligonucleotide sequences for qRT-PCR

Sequences of oligonucleotide primer sequences used for qRT-PCR in this study

Supplemental Table 18. Probe sequences

Sequences used in RNA *in situ* probes

Supplemental Table 19. Cloning Primers

Sequences of primers used in creating plasmids used in this study

Supplementary Table 20. Plasmid constructs

List of plasmid constructs used in this study

Supplemental Table 21. Activity of Cowpea promoters

Activity of cowpea promoters in *Arabidopsis thaliana*

Supplemental Data

Supplemental Data 1: IT86D-1010 genes and GO annotation

Large table with GO annotations and descriptions for all cowpea predicted genes

Supplemental Data 2: Mean RPM counts

Large table with the average RPM counts for all genes in all cell-types

Supplemental Data 3: Cell-specificity scores and RPM counts

Large set of tables with all genes in each of the cell-specific gene sets

Supplemental Data 4: Cell-specific gene annotations

Large set of tables with all cell-specific genes for each cell-type and their GO annotations

Supplemental Data 5: log2 FC2 DE genes

Large set of tables with all genes DE at log2 fold-change 2 in each of the cell-types

Supplemental Data 6: DE enriched GO terms

Large set of tables with the enriched biological process GO terms from each of DE gene sets

Supplemental Data 7: BlastP comparing Vu and At

Large table containing the best *Arabidopsis* protein match by homology to the translated coding sequence of each predicted cowpea gene

Supplemental Data 8: Raw aligned read counts

A csv file with the raw counts of aligned to each gene in each replicate.

Supplemental Data 9: Predicted gene coding sequences

A fasta file with the coding sequences of all IT86D-1010 predicted genes.

Acknowledgments

We are grateful to Tracy How and Dilrukshi Nagahatenna for their assistance with cowpea transformation and growth, to Natalia Bazanova for assistance with cloning, and to Steven Henderson for suggestions concerning the *in silico* identification of cowpea cell-specific genes.

Table 1. Genes and promoters tested for cell-type specificity by qPCR, *in situ* hybridization and transformation in cowpea.

1077

Cowpea gene or reporter construct	Arabidopsis homolog	Arabidopsis annotations / predicted localisation	Cell-type localization (*in silico* RNA-Seq)	Tissue localization by qPCR	Cell type localization by *in situ*[c]	Promoter directed gene expression in transgenic cowpea
VuMAP3K17-like	At2g32510	mitogen-activated protein kinase kinase kinase 17	MMC	MMC	-	-
VuCPK1	At5g04870	calcium dependent protein kinase 1	MMC	MMC, MIC	-	-
VuLBD12	At2g30130	Lateral organ boundaries domain family protein	fTET	fTET	-	-
Vu.g6173	At4g35670	Pectin lyase-like superfamily protein	fTET	MIC, SC	-	-
VuLHL3	At1g64625	Plant-specific basic helix-loop-helix (bHLH) protein	ES4n	ES2n/4n	-	-
Vu.g43722	At1g68040	S-adenosyl-L-methionine-dependent methyltransferases superfamily protein	ES2n	ES2n/4n	-	-
Vu.g2461	??	unknown	ES2n	ES2n/4n	-	-
VuGULL06	At2g46670	FAD-dependent oxidoreductase	CC	CC/EC	CC	-
VuNB-ARC	At3g14470	NB-ARC domain disease resistance protein	CC	fTET, ES2n/4n	CC[d]	-
VuSDR1	At3g61220	NADP-binding Rossman-fold protein	CC	NS	CC	-
VuMEE23	At2g34790	Berberine Bridge Enzyme-like protein	CC	CC/EC	CC, NC	-
VuBAS1	At2g26710	Cytochrome P450 superfamily protein	CC	CC/EC	-	-
VuEC1.1_1	At1g76750	cytosine-rich secreted protein	EC	CC/EC	EC, Sy	-
VuEC1.1_2	At1g76750	cytosine-rich secreted protein	EC	CC/EC	EC, Sy	-
VuRKD1	At1g18790	RWP-RK domain transcription factor	EC	CC/EC	EC, Sy	-
VuCAP	At3g19690	CAP superfamily protein	Em	Em	-	-
VuZFP	At5g01860	C2HC zinc fingers superfamily protein	Em	MMC, fTET, mTET, Em	-	-
VuVRN1	At3g18990	AP2/B3-like transcriptional factor family protein	Em	Roots, Petiole, Leaf, EC,Em	-	-
VuLBD13	At2g30340	LOB domain-containing protein 13	Em	Em	-	-
Vu.g56782	At4g24130	Protein of unknown function, DUF538	mTET	mTET	-	-
VuPPCK	At3g04530	phosphoenolpyruvat	mTET	mTET	-	-

		e carboxylase kinase 2				
VuXND1	At5g64530	xylem NAC domain 1	mTET	mTET	-	-
VuSRO2	At1g23550	similar to RCD one	mTET	Seedling, roots	-	-
VuXTH6	At5g65730	xyloglucan endotransglucosylase hydrolase	SC	SC	SC, VN	-
VuXTH32	At2g36870	xyloglucan endotransglucosylase hydrolase	SC	SC	SC, VC	-
VuGIM2	At2g36690	2-oxoglutarate-dependent dioxygenase	SC	SC	SC, VC	-
VuAt3g09950	At3g09950	unknown	SC	Roots, seedlings	SC, VC	-
VuKNU-like1	At5g14010	C2H2 zinc finger protein	MMC, PMC, mTET, SC	MMC, mTET, SC	MMC+NC+II	-
VuKNU-like2	At5g14010	C2H2 zinc finger protein	MMC, Em	MMC, MIC	-	-
AtRKD2 [e]	At1g74480	EC	-	-	-	EC, Em
AtEC1.1 [e]	At1g76750	EC	-	-	-	EC
AtDD45 [e]	At2g21740	EC	-	-	-	EC
AtDD1 [e]	At1g36340	AC	-	-	-	non-specific
AtDD9 [e]	At1g26795	CC	-	-	-	CC
AtDD25 [e]	At3g04540	CC	-	-	-	CC
AtDD65 [e]	At3g10890	CC	-	-	-	ND
AtDD31 [e]	At1g47470	SC	-	-	-	ND
AtDUO1 [e]	At3g60460	SC	-	-	-	ND
AtLAT52 [e]	At5g45880	VC	-	-	-	ND
AtKNU [e]	At5g14010	MMC + PMC	-	-	-	MMC, PMC, II

Footnotes

[a] Based on *Arabidopsis thaliana* genome annotation TAIR 10.

[b] Based on laser-capture cell transcriptomes

[c] Based on *in situ* hybridization

[d] Shows nuclear dots corresponding to active transcription in the central cell nuclei

[e] Fluorescent reporter gene constructs

Abbreviations: CC, central cell; EC, egg cell; II, inner ovule integument; MMC, megaspore mother cell; NC, nucellar cells; SC, sperm cell; Sy, synergid; VC, vegetative cell; VN, vegetative nucleus.

Table 2. The number of genes upregulated in each cell-type compared to the average expression in all cell-types.

Cell type	Number of genes differentially upregulated
MMC	5878
fTET	2316
ES2n	2627
ES4n	1423
CC	1897
EC	1550
MES	3376
Em	5051
PMC E	1282
PMC L	2653
mTET	3743
MIC	3101
sperm	38691
Leaf	9140

Figure Legends

Figure 1. Stages of reproductive development in cowpea and gene expression in developed transcriptomes.

A, Cartoon of temporal stages of male and female gametophyte development showing cell-type stages collected by LCM for RNAseq. For detail refer to text. B, The number of genes expressed in each transcriptome set (RPM >0). C, The proportion of genes expressed at very low (<1RPM), low (1-5RPM), moderate (5-20RPM) or high (>20RPM) levels in RNAseq sets. Abbreviations: MMC, megaspore mother cell; fTET, female tetrads; FM, functional megaspore selection stage (not collected); ES2n, mitotic embryo sac with 2 nuclei; ES4n, embryo sac with 4 nuclei; MES, mature embryo sac at anthesis, where antipodals have degenerated, containing the egg cell (EC), flanking synergids (Sy, not collected), and central cell (CC); Em, embryo; En, endosperm (not collected); PMC.E, early pollen mother cell; PMC.L, late pollen mother cell; mTET, male tetrads; MIC, uninucleate microspore; Bi, bicellular pollen stage; Tri, tricellular pollen stage, two sperm cells (SC) in the emerging pollen tube; MP-SC, mature pollen-sperm cell.

Figure 2. Gene expression in cowpea reproductive cell-types**.**

A – J, Whole-mount *in situ* hybridization (WISH) in pollen grains of cowpea using four different antisense probes. A-C, *VuXTH6* mRNA in sperm cells A and vegetative nucleus B, with no signal in the sense control C. D and E, *VuXTH32* mRNA was detected in sperm cell and vegetative cell cytoplasm. F, *VuXTH32* sense controls. G, Whole-mount ovule undergoing megasporogenesis showing *VuKNU1* mRNA localized in the MMC, the nucellus and the inner integument. H, Paraffin section through a differentiated female gametophyte showing

VuRKD1 mRNA localization in the egg cell and synergids. I, Paraffin section through a differentiated female gametophyte showing *VuNB-ARC* mRNA localization in the central cell. Inset shows fused polar nuclei showing active transcription of *VuNB-ARC*. J, *AtRKD2*$_{pro}$*:dsRED-Express* (red) in EC and *AtDD9*$_{pro}$*:AmCyan1* (cyan) in the CC one day before anthesis. K, *AtEC1.1*$_{pro}$*:AmCyan1* (cyan) in EC and *AtDD25*$_{pro}$*:dsRED-Express* (red) in CC. L-M, *AtDD45*$_{pro}$*:dsRED-Express* (red) in an isolated egg cell, N, two-celled proembryo and O, early embryo.

Abbreviations: EC, egg cell; CC, central cell; Sy, synergids; SC, sperm cells; VN, vegetative nucleus, MMC, megaspore mother cell.

Scale bars: A-G, L-M = 10 µm, H = 8 µm, I = 14 µm, J-K = 50 µm, N-O = 20 µm.

Figure 3. Differentially enriched Biological Process GO terms and expression of meiosis genes during gametogenesis.

A, Enriched GO terms primarily in female gametophyte and early embryo transcriptomes. B, Enriched GO terms primarily in the male gametophyte and leaf transcriptomes. The statistical significance of the GO enrichment is represented according to the scale of weighted Fisher p value shown at the bottom right. C, Expression of genes involved in meiosis in the generated cowpea transcriptomes (See also Supplemental Tables 7 and 8). Expression levels relate to the RPM scale.

Figure 4. Expression of auxin biosynthesis and auxin responsive genes during meiosis and gametophyte development.

A, Expression of genes belonging to the YUCCA and TAR auxin biosynthesis families. B, Expression of 60 auxin responsive genes sorted in decreasing order of expression level in the

2-nucleate embryo sac. Expression levels are related to the RPM scale with each respective panel. (See also Supplemental Table 9).

Figure 5. Heatmaps representing the expression of selected genes involved in RNA-mediated gene silencing and DNA methylation.

A, Expression of genes involved in the miRNA-mediated gene silencing pathway and in PTGS. B, Expression of genes that interact with RNA and are involved in RdDM, DNA methyltransferases that mediate RdDM and DNA glycosylases that mediate demethylation of DNA. Expression level is according to the RPM scales for each panel. (See also Supplemental Tables 12 and 13).

Figure 6. Histone gene expression and the expression of selected genes involved in histone modification.

A, Expression of genes belonging to the core histone family (See Supplementary Table 18). B, Expression of selected PcG genes involved in histone methylation resulting in gene silencing (See Supplementary Table 19). C, Known protein interactions forming Polycomb-group repressive 2 complex types. Accessory proteins (X) are often associated with PRC2 complex function. Asterisks indicate *Arabidopsis* specific proteins. MEA and *Arabidopsis* counterparts, SWN and CLF are SET domain proteins and homologs of *Drosophilia* Enhancer of Zeste. FIS2 and others listed are VEFS-box proteins. FIE and MSI1 are WD40 repeat protein containing proteins (Mozgova and Henning, 2015). D, Expression of selected JMJ family histone demethylase genes and demethylation targets, at left (See also Supplemental Tables 14, 15, 16). Expression levels relate to the RPM scales associated with each panel.

Figure 7. Expression of selected cell cycle genes in egg, central cell, mature pollen-sperm and leaf transcriptomes.

Cell cycle genes are grouped according to their function relating to roles in promoting or blocking progression through various cell cycle phases. Relative expression level is indicated according to the RPM scale shown at the bottom of each panel. (See also Supplemental Tables 10 and 11).

Supplemental Figure. 1. Correlation between RNAseq replicates.

Scatter plot of log-transformed mean RPM counts of replicates for each tissue. Replicate 1 and replicate 2 for each cell-type are shown on the Y and X axes, respectively.

Supplemental Figure. 2. Principal component analysis (PCA).

PCA plot showing relationships between all transcriptomes.

Abbreviations: MMC, megaspore mother cell; fTET, female tetrads; ES2n, mitotic embryo sac with 2 nuclei; ES4n, embryo sac with 4 nuclei; MES, mature embryo sac at anthesis, containing the egg cell (EC) and central cell (CC); Em, embryo; PMC.E, early pollen mother cell; PMC.L, late pollen mother cell; mTET, male tetrads; MIC, uninucleate microspore; MP-SC, mature pollen-sperm cell.

Supplemental Figure. 3. Cell-specific genes expression

Heat-map of scaled RPM expression values of the cell-specific genes identified using the rsgcc software package

Supplemental Figure. 4. *In situ* hybridization of cell-specific cowpea genes in gametophytic tissue and fluorescent reporters expressed from *Arabidopsis* cell-specific promoters in cowpea.

A-B, *VuXTH32* mRNA localized in the sperm cells and vegetative cell cytoplasm. C, *VuXTH32* sense control. D-E, *VuAt3g09950* mRNA abundantly localized in the sperm and vegetative cells. F, sense *VuAt3g09950* control. G, Paraffin section through a fully differentiated female gametophyte showing *VuEC1.1* mRNA localization in the egg cell. H, Consecutive section to (G) showing *VuEC1.1* mRNA localization in the synergids. I, Detail of G showing mRNA localization in the egg cell. J, Detail of H showing mRNA localization in the synergids. K, Whole-mounted ovule showing *VuMEE23* mRNA localization in the central cell and adjacent nucellar cells. L-M, $AtDUO1_{pro}$*:AcGFP1* no expression. N, Whole-mounted ovule showing *VuSDR1* mRNA localization in the central cell. O, Whole-mounted ovule showing *VuGULL06* mRNA localization confined to the central cell. P, No expression of $AtLAT52_{pro}$*:AcGFP1* in germinating pollen. Q, Mature female gametophyte with egg cell, polar nuclei and central cell in cleared ovule. R, $AtDD45_{pro}$*:dsRED-Express* (red) in EC and general pattern of the $AtDD1_{pro}$*:ZsYellow1* (yellow) in cells external to the embryo sac and in CC. S, $AtEC1.1_{pro}$*:AmCyan1* (cyan) in zygote and $AtDD25_{pro}$*:dsRED-Express* (red) in early endosperm. T, $AtRKD2_{pro}$*:dsRED-Express* (red) in zygote and $AtDD9_{pro}$*:AmCyan1* (cyan) in early endosperm. U, $AtRKD2_{pro}$*:dsRED-Express* in early embryo. *AtDD9* is not expressed at this stage. V, Cleared ovule showing early embryo corresponding to the stage in U.

Scale bars: A-F, I-J = 10 µm; G-H = 18 µm; K, N-O = 35 µm; L-M, P-T = 50 µm; U-V = 100 µm

Abbreviations: EC, egg cell; CC, central cell; Sy, synergids; SC, sperm cells; VN, vegetative nucleus; PN, polar nuclei; Em, embryo; En, endosperm; Zy, zygote.

Supplemental Figure. 5. Expression of the KNU genes in cowpea.

A, Whole-mount pre-meiotic ovule showing *VuKNU1* mRNA localized in the MMC and the developing nucellus at the onset of integument initiation. B-D, Micrographs of cowpea ovules expressing a *AtKNU$_{pro}$:nlsYFP* reporter construct marking MMC fate. E-F, At the end of meiosis the KNU promoter turns off in female functional megaspore, but the expression persists in somatic ovule cells at the chalazal end. G-H, Expression of *AtKNU$_{pro}$:nlsYFP* reporter construct during male meiosis. I, Male tetrad showing no expression of reporter construct. J, After the first pollen mitosis, the expression of reporter construct is evident in both vegetative and generative nucleus. K, Mature pollen grain does not show any expression.

Abbreviations: MMC, megaspore mother cell; GC, generative cell; VN, vegetative nucleus.

Scale bars: A = 10 µm; B = 100 µm; C-H = 50 µm; I-K = 20 µm.

Supplemental Figure. 6. Specific activity of cowpea promoters in reproductive cells of *Arabidopsis thaliana*. A, *VuKNU-L1$_{pro}$:GUS* expression in the developing ovule of *Arabidopsis*. B, *VuRKD1$_{pro}$:GUS* expression in the egg cell. C, *VuRKD1$_{pro}$:GUS* expression in a sperm cell. D, *VuRKD1$_{pro}$:GUS* expression in the vegetative cell. E, *VuGULL06$_{pro}$:GUS* in the egg apparatus. F, *VuXTH32$_{pro}$:GUS* expression in the vegetative cell. G, *VuGIM2$_{pro}$:GUS* expression in the vegetative cell. Scale Bars: A, F, and G = 10 µm; B and D = 20 µm; C and D = 8 µm.

Supplemental Figure. 7. Phylogeny of the AGO family in cowpea and *Arabidopsis*

A Jukes-Cantor Neighbour-Joining consensus tree showing the relationship between the AGO genes identified in cowpea (Vu) and those known in *Arabidopsis* (At).

Parameters for tree building were ClustalW MSA with BLOSUM cost matrix, Gap open cost 10, Gap extend cost 0.1. Jukes-Cantor Neighbour-Joining consensus tree, no outgroup, Bootstrap resampling with 1000 replicates, 50% support threshold.

Supplemental Figure. 8. Phylogeny of *Arabidopsis* and cowpea histone proteins

Jukes-Cantor Neighbour-Joining consensus tree showing the relationship between the *Arabidopsis* and cowpea histones is shown. Histone1 (orange), Histone2 (blue), Histone3 (green), Histone4 (pink), CenH3 (yellow). A Parameters for tree building were ClustalW MSA with BLOSUM cost matrix, Gap open cost 10, Gap extend cost 0.1. Jukes-Cantor Neighbour-Joining consensus tree, no outgroup, Bootstrap resampling with 1000 replicates, 50% support threshold.

Literature Cited

ANDERSON, S. N., JOHNSON, C. S., JONES, D. S., CONRAD, L. J., GOU, X., RUSSELL, S. D. & SUNDARESAN, V. 2013. Transcriptomes of isolated Oryza sativa gametes characterized by deep sequencing: evidence for distinct sex-dependent chromatin and epigenetic states before fertilization. *Plant J,* 76**,** 729-41.

ASHBURNER, M., BALL, C. A., BLAKE, J. A., BOTSTEIN, D., BUTLER, H., CHERRY, J. M., DAVIS, A. P., DOLINSKI, K., DWIGHT, S. S., EPPIG, J. T., HARRIS, M. A., HILL, D. P., ISSEL-TARVER, L., KASARSKIS, A., LEWIS, S., MATESE, J. C., RICHARDSON, J. E., RINGWALD, M., RUBIN, G. M. & SHERLOCK, G. 2000. Gene ontology: tool for the unification of biology. The Gene Ontology Consortium. *Nat Genet,* 25**,** 25-9.

BARTRINA, I., OTTO, E., STRNAD, M., WERNER, T. & SCHMULLING, T. 2011. Cytokinin regulates the activity of reproductive meristems, flower organ size, ovule formation, and thus seed yield in Arabidopsis thaliana. *Plant Cell,* 23**,** 69-80.

BASS, H. W., MARSHALL, W. F., SEDAT, J. W., AGARD, D. A. & CANDE, W. Z. 1997. Telomeres cluster de novo before the initiation of synapsis: a three-dimensional spatial analysis of telomere positions before and during meiotic prophase. *J Cell Biol,* 137**,** 5-18.

BELMONTE, M. F., KIRKBRIDE, R. C., STONE, S. L., PELLETIER, J. M., BUI, A. Q., YEUNG, E. C., HASHIMOTO, M., FEI, J., HARADA, M., MUNOZ, M. D., LE, B. H., DREWS, G. N., BRADY, S. M., GOLDBERG, R. B. & HARADA, J. J. 2013. Comprehensive developmental

profiles of gene activity in regions and subregions of the Arabidopsis seed. *Proceedings of the National Academy of Sciences of the United States of America,* 110, E435-E444.

BERGER, F., HAMAMURA, Y., INGOUFF, M. & HIGASHIYAMA, T. 2008. Double fertilization - caught in the act. *Trends Plant Sci,* 13, 437-43.

BORG, M. & BERGER, F. 2015. Chromatin remodelling during male gametophyte development. *Plant J,* 83, 177-88.

BORGES, F. & MARTIENSSEN, R. A. 2015. The expanding world of small RNAs in plants. *Nature Reviews Molecular Cell Biology,* 16, 727-741.

BREWBAKER, J. L. 1967. THE DISTRIBUTION AND PHYLOGENETIC SIGNIFICANCE OF BINUCLEATE AND TRINUCLEATE POLLEN GRAINS IN THE ANGIOSPERMS. *American Journal of Botany,* 54, 1069-1083.

BREWBAKER, J. L. & KWACK, B. H. 1963. THE ESSENTIAL ROLE OF CALCIUM ION IN POLLEN GERMINATION AND POLLEN TUBE GROWTH. *American Journal of Botany,* 50, 859-865.

BUCHFINK, B., XIE, C. & HUSON, D. H. 2015. Fast and sensitive protein alignment using DIAMOND. *Nat Methods,* 12, 59-60.

CHEN, J., STRIEDER, N., KROHN, N. G., CYPRYS, P., SPRUNCK, S., ENGELMANN, J. C. & DRESSELHAUS, T. 2017. Zygotic Genome Activation Occurs Shortly after Fertilization in Maize. *Plant Cell,* 29, 2106-2125.

CLOUGH, S. J. & BENT, A. F. 1998. Floral dip: a simplified method for Agrobacterium-mediated transformation of Arabidopsis thaliana. *Plant J,* 16, 735-43.

CROMER, L., HEYMAN, J., TOUATI, S., HARASHIMA, H., ARAOU, E., GIRARD, C., HORLOW, C., WASSMANN, K., SCHNITTGER, A., DE VEYLDER, L. & MERCIER, R. 2012. OSD1 promotes meiotic progression via APC/C inhibition and forms a regulatory network with TDM and CYCA1;2/TAM. *PLoS Genet,* 8, e1002865.

CURTIS, M. D. & GROSSNIKLAUS, U. 2003. A gateway cloning vector set for high-throughput functional analysis of genes in planta. *Plant Physiol,* 133, 462-9.

DANTE, R. A., LARKINS, B. A. & SABELLI, P. A. 2014. Cell cycle control and seed development. *Front Plant Sci,* 5, 493.

DE SCHUTTER, K., JOUBES, J., COOLS, T., VERKEST, A., CORELLOU, F., BABIYCHUK, E., VAN DER SCHUEREN, E., BEECKMAN, T., KUSHNIR, S., INZE, D. & DE VEYLDER, L. 2007. Arabidopsis WEE1 kinase controls cell cycle arrest in response to activation of the DNA integrity checkpoint. *Plant Cell,* 19, 211-25.

DENG, L., ZHANG, S., WANG, G., FAN, S., LI, M., CHEN, W., TU, B., TAN, J., WANG, Y., MA, B., LI, S. & QIN, P. 2017. Down-Regulation of OsEMF2b Caused Semi-sterility Due to Anther and Pollen Development Defects in Rice. *Front Plant Sci,* 8, 1998.

FAN, D., WANG, X., TANG, X., YE, X., REN, S., WANG, D. & LUO, K. 2018. Histone H3K9 demethylase JMJ25 epigenetically modulates anthocyanin biosynthesis in poplar. *Plant J,* 96, 1121-1136.

FRIEDMAN, W. E. 1999. Expression of the cell cycle in sperm of Arabidopsis: implications for understanding patterns of gametogenesis and fertilization in plants and other eukaryotes. *Development,* 126, 1065-1075.

GARCÍA-AGUILAR, M., DORANTES-ACOSTA, A., PÉREZ-ESPAÑA, V. & VIELLE-CALZADA, J.-P. 2005. Whole-mount in situ mRNA localization in developing ovules and seeds ofArabidopsis. *Plant Molecular Biology Reporter,* 23, 279-289.

GIBSON, S. W. & TODD, C. D. 2015. Arabidopsis AIR12 influences root development. *Physiol Mol Biol Plants,* 21**,** 479-89.

GREEN-ARMYTAGE, P. 2010. A Colour Alphabet and the Limits of Colour Coding. *Colour: Design & Creativity,* 5**,** 1-23.

GROSSNIKLAUS, U. & PARO, R. 2014. Transcriptional silencing by polycomb-group proteins. *Cold Spring Harb Perspect Biol,* 6**,** a019331.

HAERIZADEH, F., WONG, C. E., BHALLA, P. L., GRESSHOFF, P. M. & SINGH, M. B. 2009. Genomic expression profiling of mature soybean (Glycine max) pollen. *BMC Plant Biol,* 9**,** 25.

HAGA, N., KOBAYASHI, K., SUZUKI, T., MAEO, K., KUBO, M., OHTANI, M., MITSUDA, N., DEMURA, T., NAKAMURA, K., JURGENS, G. & ITO, M. 2011. Mutations in MYB3R1 and MYB3R4 cause pleiotropic developmental defects and preferential down-regulation of multiple G2/M-specific genes in Arabidopsis. *Plant Physiol,* 157**,** 706-17.

HANDS, P., RABIGER, D. S. & KOLTUNOW, A. 2016. Mechanisms of endosperm initiation. *Plant Reprod,* 29**,** 215-25.

HUANG, K. L., MA, G. J., ZHANG, M. L., XIONG, H., WU, H., ZHAO, C. Z., LIU, C. S., JIA, H. X., CHEN, L., KJORVEN, J. O., LI, X. B. & REN, F. 2018. The ARF7 and ARF19 Transcription Factors Positively Regulate PHOSPHATE STARVATION RESPONSE1 in Arabidopsis Roots. *Plant Physiol,* 178**,** 413-427.

IBARRA, C. A., FENG, X., SCHOFT, V. K., HSIEH, T. F., UZAWA, R., RODRIGUES, J. A., ZEMACH, A., CHUMAK, N., MACHLICOVA, A., NISHIMURA, T., ROJAS, D., FISCHER, R. L., TAMARU, H. & ZILBERMAN, D. 2012. Active DNA demethylation in plant companion cells reinforces transposon methylation in gametes. *Science,* 337**,** 1360-1364.

JACKSON, D. 1992. In-Situ Hybridization in Plants. *In:* GURR, S. J., MCPHERSON, M. J. & BOWLES, D. J. (eds.) *Molecular Plant Pathology: A Practical Approach* Oxford University Press.

JURANIC, M., TUCKER, M. R., SCHULTZ, C. J., SHIRLEY, N. J., TAYLOR, J. M., SPRIGGS, A., JOHNSON, S. D., BULONE, V. & KOLTUNOW, A. M. 2018. Asexual Female Gametogenesis Involves Contact with a Sexually-Fated Megaspore in Apomictic Hieracium. *Plant Physiol,* 177**,** 1027-1049.

KAWASHIMA, T. & BERGER, F. 2014. Epigenetic reprogramming in plant sexual reproduction. *Nat Rev Genet,* 15**,** 613-24.

KIM, T. W., HWANG, J. Y., KIM, Y. S., JOO, S. H., CHANG, S. C., LEE, J. S., TAKATSUTO, S. & KIM, S. K. 2005. Arabidopsis CYP85A2, a cytochrome P450, mediates the Baeyer-Villiger oxidation of castasterone to brassinolide in brassinosteroid biosynthesis. *Plant Cell,* 17**,** 2397-412.

KLEPIKOVA, A. V., KASIANOV, A. S., GERASIMOV, E. S., LOGACHEVA, M. D. & PENIN, A. A. 2016. A high resolution map of the Arabidopsis thaliana developmental transcriptome based on RNA-seq profiling. *Plant J,* 88**,** 1058-1070.

KOBAYASHI, K., SUZUKI, T., IWATA, E., MAGYAR, Z., BOGRE, L. & ITO, M. 2015. MYB3Rs, plant homologs of Myb oncoproteins, control cell cycle-regulated transcription and form DREAM-like complexes. *Transcription,* 6**,** 106-11.

KOMAKI, S. & SUGIMOTO, K. 2012. Control of the plant cell cycle by developmental and environmental cues. *Plant Cell Physiol,* 53**,** 953-64.

KOSZEGI, D., JOHNSTON, A. J., RUTTEN, T., CZIHAL, A., ALTSCHMIED, L., KUMLEHN, J., WUST, S. E., KIRIOUKHOVA, O., GHEYSELINCK, J., GROSSNIKLAUS, U. & BAUMLEIN, H. 2011.

Members of the RKD transcription factor family induce an egg cell-like gene expression program. *Plant J,* 67**,** 280-91.

KUBO, T., FUJITA, M., TAKAHASHI, H., NAKAZONO, M., TSUTSUMI, N. & KURATA, N. 2013. Transcriptome analysis of developing ovules in rice isolated by laser microdissection. *Plant Cell Physiol,* 54**,** 750-65.

LAWIT, S. J., CHAMBERLIN, M. A., AGEE, A., CASWELL, E. S. & ALBERTSEN, M. C. 2013. Transgenic manipulation of plant embryo sacs tracked through cell-type-specific fluorescent markers: cell labeling, cell ablation, and adventitious embryos. *Plant Reproduction,* 26**,** 125-137.

LI, L., ZHAO, Y. F., MCCAIG, B. C., WINGERD, B. A., WANG, J. H., WHALON, M. E., PICHERSKY, E. & HOWE, G. A. 2004. The tomato homolog of CORONATINE-INSENSITIVE1 is required for the maternal control of seed maturation, jasmonate-signaled defense responses, and glandular trichome development (vol 16, pg 126, 2004). *Plant Cell,* 16**,** 783-783.

LITUIEV, D. S., KROHN, N. G., MULLER, B., JACKSON, D., HELLRIEGEL, B., DRESSELHAUS, T. & GROSSNIKLAUS, U. 2013. Theoretical and experimental evidence indicates that there is no detectable auxin gradient in the angiosperm female gametophyte. *Development,* 140**,** 4544-4553.

LIU, P., ZHANG, S., ZHOU, B., LUO, X., ZHOU, X. F., CAI, B., JIN, Y. H., NIU, LIN, J., CAO, X. & JIN, J. B. 2019. The Histone H3K4 Demethylase JMJ16 Represses Leaf Senescence in Arabidopsis. *Plant Cell,* 31**,** 430-443.

LONARDI, S., MUNOZ-AMATRIAIN, M., LIANG, Q., SHU, S., WANAMAKER, S. I., LO, S., TANSKANEN, J., SCHULMAN, A. H., ZHU, T., LUO, M. C., ALHAKAMI, H., OUNIT, R., HASAN, A. M., VERDIER, J., ROBERTS, P. A., SANTOS, J. R. P., NDEVE, A., DOLEZEL, J., VRANA, J., HOKIN, S. A., FARMER, A. D., CANNON, S. B. & CLOSE, T. J. 2019. The genome of cowpea (Vigna unguiculata [L.] Walp.). *Plant J,* 98**,** 767-782.

LOVE, M. I., HUBER, W. & ANDERS, S. 2014. Moderated estimation of fold change and dispersion for RNA-seq data with DESeq2. *Genome Biol,* 15**,** 550.

MA, C. & WANG, X. 2012. Application of the Gini correlation coefficient to infer regulatory relationships in transcriptome analysis. *Plant Physiol,* 160**,** 192-203.

MARTINEZ, G., PANDA, K., KOHLER, C. & SLOTKIN, R. K. 2016. Silencing in sperm cells is directed by RNA movement from the surrounding nurse cell. *Nat Plants,* 2**,** 16030.

MOGENSEN, H. L. & HOLM, P. B. 1995. Dynamics of Nuclear-DNA Quantities during Zygote Development in Barley. *Plant Cell,* 7**,** 487-494.

MOZGOVA, I. & HENNIG, L. 2015. The polycomb group protein regulatory network. *Annu Rev Plant Biol,* 66**,** 269-96.

MUNOZ-AMATRIAIN, M., MIREBRAHIM, H., XU, P., WANAMAKER, S. I., LUO, M., ALHAKAMI, H., ALPERT, M., ATOKPLE, I., BATIENO, B. J., BOUKAR, O., BOZDAG, S., CISSE, N., DRABO, I., EHLERS, J. D., FARMER, A., FATOKUN, C., GU, Y. Q., GUO, Y. N., HUYNH, B. L., JACKSON, S. A., KUSI, F., LAWLEY, C. T., LUCAS, M. R., MA, Y., TIMKO, M. P., WU, J., YOU, F., BARKLEY, N. A., ROBERTS, P. A., LONARDI, S. & CLOSE, T. J. 2017. Genome resources for climate-resilient cowpea, an essential crop for food security. *Plant J,* 89**,** 1042-1054.

OKADA, T., HU, Y. K., TUCKER, M. R., TAYLOR, J. M., JOHNSON, S. D., SPRIGGS, A., TSUCHIYA, T., OELKERS, K., RODRIGUES, J. C. M. & KOLTUNOW, A. M. G. 2013. Enlarging Cells Initiating Apomixis in Hieracium praealtum Transition to an Embryo Sac Program prior to Entering Mitosis. *Plant Physiology,* 163**,** 216-231.

1395 OLMEDO-MONFIL, V., DURAN-FIGUEROA, N., ARTEAGA-VAZQUEZ, M., DEMESA-AREVALO,
1396 E., AUTRAN, D., GRIMANELLI, D., SLOTKIN, R. K., MARTIENSSEN, R. A. & VIELLE-
1397 CALZADA, J. P. 2010. Control of female gamete formation by a small RNA pathway in
1398 Arabidopsis. *Nature,* 464**,** 628-32.
1399 PAGNUSSAT, G. C., ALANDETE-SAEZ, M., BOWMAN, J. L. & SUNDARESAN, V. 2009. Auxin-
1400 Dependent Patterning and Gamete Specification in the Arabidopsis Female
1401 Gametophyte. *Science,* 324**,** 1684-1689.
1402 PANOLI, A., MARTIN, M. V., ALANDETE-SAEZ, M., SIMON, M., NEFF, C., SWARUP, R.,
1403 BELLIDO, A., YUAN, L., PAGNUSSAT, G. C. & SUNDARESAN, V. 2015. Auxin Import and
1404 Local Auxin Biosynthesis Are Required for Mitotic Divisions, Cell Expansion and Cell
1405 Specification during Female Gametophyte Development in Arabidopsis thaliana. *Plos*
1406 *One,* 10.
1407 PAYNE, T., JOHNSON, S. D. & KOLTUNOW, A. M. 2004. KNUCKLES (KNU) encodes a C2H2
1408 zinc-finger protein that regulates development of basal pattern elements of the
1409 Arabidopsis gynoecium. *Development,* 131**,** 3737-49.
1410 PEGLER, J. L., OULTRAM, J. M. J., GROF, C. P. L. & EAMENS, A. L. 2019. Profiling the Abiotic
1411 Stress Responsive microRNA Landscape of Arabidopsis thaliana. *Plants (Basel),* 8.
1412 PENTERMAN, J., ZILBERMAN, D., HUH, J. H., BALLINGER, T., HENIKOFF, S. & FISCHER, R. L.
1413 2007. DNA demethylation in the Arabidopsis genome. *Proceedings of the National*
1414 *Academy of Sciences of the United States of America,* 104**,** 6752-6757.
1415 PIEN, S. & GROSSNIKLAUS, U. 2007. Polycomb group and trithorax group proteins in
1416 Arabidopsis. *Biochim Biophys Acta,* 1769**,** 375-82.
1417 PILLOT, M., AUTRAN, D., LEBLANC, O. & GRIMANELLI, D. 2010. A role for
1418 CHROMOMETHYLASE3 in mediating transposon and euchromatin silencing during
1419 egg cell reprogramming in Arabidopsis. *Plant Signal Behav,* 5**,** 1167-70.
1420 POPELKA, J. C., GOLLASCH, S., MOORE, A., MOLVIG, L. & HIGGINS, T. J. V. 2006. Genetic
1421 transformation of cowpea (Vigna unguiculata L.) and stable transmission of the
1422 transgenes to progeny. *Plant Cell Reports,* 25**,** 304-312.
1423 RAMAKERS, C., RUIJTER, J. M., DEPREZ, R. H. L. & MOORMAN, A. F. M. 2003. Assumption-
1424 free analysis of quantitative real-time polymerase chain reaction (PCR) data.
1425 *Neuroscience Letters,* 339**,** 62-66.
1426 RAY, S., AGARWAL, P., ARORA, R., KAPOOR, S. & TYAGI, A. K. 2007. Expression analysis of
1427 calcium-dependent protein kinase gene family during reproductive development and
1428 abiotic stress conditions in rice (Oryza sativa L. ssp. indica). *Mol Genet Genomics,*
1429 278**,** 493-505.
1430 RUIJTER, J. M., RAMAKERS, C., HOOGAARS, W. M. H., KARLEN, Y., BAKKER, O., VAN DEN
1431 HOFF, M. J. B. & MOORMAN, A. F. M. 2009. Amplification efficiency: linking baseline
1432 and bias in the analysis of quantitative PCR data. *Nucleic Acids Research,* 37.
1433 RUTLEY, N. & TWELL, D. 2015. A decade of pollen transcriptomics. *Plant Reproduction,* 28**,**
1434 73-89.
1435 SALINAS-GAMBOA, R., JOHNSON, S. D., SANCHEZ-LEON, N., KOLTUNOW, A. M. G. & VIELLE-
1436 CALZADA, J. P. 2016. New observations on gametogenic development and
1437 reproductive experimental tools to support seed yield improvement in cowpea
1438 [Vigna unguiculata (L.) Walp.]. *Plant Reproduction,* 29**,** 165-177.
1439 SCHMIDT, A., WUEST, S. E., VIJVERBERG, K., BAROUX, C., KLEEN, D. & GROSSNIKLAUS, U.
1440 2011. Transcriptome analysis of the Arabidopsis megaspore mother cell uncovers the

1441 importance of RNA helicases for plant germline development. *PLoS Biol,* 9,
1442 e1001155.
1443 SCHOFT, V. K., CHUMAK, N., CHOI, Y., HANNON, M., GARCIA-AGUILAR, M., MACHLICOVA, A.,
1444 SLUSARZ, L., MOSIOLEK, M., PARK, J. S., PARK, G. T., FISCHER, R. L. & TAMARU, H.
1445 2011. Function of the DEMETER DNA glycosylase in the Arabidopsis thaliana male
1446 gametophyte. *Proc Natl Acad Sci U S A,* 108, 8042-7.
1447 SCOFIELD, S., JONES, A. & MURRAY, J. A. 2014. The plant cell cycle in context. *J Exp Bot,* 65,
1448 2557-62.
1449 SHERMOEN, A. W. & O'FARRELL, P. H. 1991. Progression of the Cell-Cycle through Mitosis
1450 Leads to Abortion of Nascent Transcripts. *Cell,* 67, 303-310.
1451 SINGH, B. B. 2014. Cowpea: The Food Legume of the 21st Century. *Cowpea: The Food*
1452 *Legume of the 21st Century*, 1-170.
1453 SLOTKIN, R. K., VAUGHN, M., BORGES, F., TANURDZIC, M., BECKER, J. D., FEIJO, J. A. &
1454 MARTIENSSEN, R. A. 2009. Epigenetic reprogramming and small RNA silencing of
1455 transposable elements in pollen. *Cell,* 136, 461-72.
1456 SORNAY, E., FORZANI, C., FORERO-VARGAS, M., DEWITTE, W. & MURRAY, J. A. 2015.
1457 Activation of CYCD7;1 in the central cell and early endosperm overcomes cell-cycle
1458 arrest in the Arabidopsis female gametophyte, and promotes early endosperm and
1459 embryo development. *Plant J,* 84, 41-55.
1460 SPRIGGS, A., HENDERSON, S. T., HAND, M. L., JOHNSON, S. D., TAYLOR, J. M. & KOLTUNOW,
1461 A. 2018. Assembled genomic and tissue-specific transcriptomic data resources for
1462 two genetically distinct lines of Cowpea (Vigna unguiculata (L.) Walp). *Gates Open*
1463 *Res,* 2, 7.
1464 SPRUNCK, S., RADEMACHER, S., VOGLER, F., GHEYSELINCK, J., GROSSNIKLAUS, U. &
1465 DRESSELHAUS, T. 2012. Egg cell-secreted EC1 triggers sperm cell activation during
1466 double fertilization. *Science,* 338, 1093-7.
1467 STANKE, M. & WAACK, S. 2003. Gene prediction with a hidden Markov model and a new
1468 intron submodel. *Bioinformatics,* 19 Suppl 2, ii215-25.
1469 STEFFEN, J. G., KANG, I. H., MACFARLANE, J. & DREWS, G. N. 2007. Identification of genes
1470 expressed in the Arabidopsis female gametophyte. *Plant J,* 51, 281-92.
1471 SUKAWA, Y. & OKAMOTO, T. 2018. Cell cycle in egg cell and its progression during zygotic
1472 development in rice. *Plant Reprod,* 31, 107-116.
1473 SUN, Q. & ZHOU, D. X. 2008. Rice jmjC domain-containing gene JMJ706 encodes H3K9
1474 demethylase required for floral organ development. *Proc Natl Acad Sci U S A,* 105,
1475 13679-84.
1476 TALBERT, P. B., AHMAD, K., ALMOUZNI, G., AUSIO, J., BERGER, F., BHALLA, P. L., BONNER, W.
1477 M., CANDE, W. Z., CHADWICK, B. P., CHAN, S. W. L., CROSS, G. A. M., CUI, L. W.,
1478 DIMITROV, S. I., DOENECKE, D., EIRIN-LOPEZ, J. M., GOROVSKY, M. A., HAKE, S. B.,
1479 HAMKALO, B. A., HOLEC, S., JACOBSEN, S. E., KAMIENIARZ, K., KHOCHBIN, S.,
1480 LADURNER, A. G., LANDSMAN, D., LATHAM, J. A., LOPPIN, B., MALIK, H. S.,
1481 MARZLUFF, W. F., PEHRSON, J. R., POSTBERG, J., SCHNEIDER, R., SINGH, M. B.,
1482 SMITH, M. M., THOMPSON, E., TORRES-PADILLA, M. E., TREMETHICK, D. J., TURNER,
1483 B. M., WATERBORG, J. H., WOLLMANN, H., YELAGANDULA, R., ZHU, B. & HENIKOFF,
1484 S. 2012. A unified phylogeny-based nomenclature for histone variants. *Epigenetics &*
1485 *Chromatin,* 5.
1486 THE GENE ONTOLOGY, C. 2017. Expansion of the Gene Ontology knowledgebase and
1487 resources. *Nucleic Acids Res,* 45, D331-D338.

TUCKER, M. R., OKADA, T., HU, Y., SCHOLEFIELD, A., TAYLOR, J. M. & KOLTUNOW, A. M. 2012. Somatic small RNA pathways promote the mitotic events of megagametogenesis during female reproductive development in Arabidopsis. *Development,* 139**,** 1399-404.

VELAPPAN, Y., SIGNORELLI, S. & CONSIDINE, M. J. 2017. Cell cycle arrest in plants: what distinguishes quiescence, dormancy and differentiated G1? *Ann Bot,* 120**,** 495-509.

VIELLE-CALZADA, J. P., BASKAR, R. & GROSSNIKLAUS, U. 2000. Delayed activation of the paternal genome during seed development. *Nature,* 404**,** 91-4.

VIELLE-CALZADA, J. P., THOMAS, J., SPILLANE, C., COLUCCIO, A., HOEPPNER, M. A. & GROSSNIKLAUS, U. 1999. Maintenance of genomic imprinting at the Arabidopsis medea locus requires zygotic DDM1 activity. *Genes & Development,* 13**,** 2971-2982.

WANG, G. & KOHLER, C. 2017. Epigenetic processes in flowering plant reproduction. *J Exp Bot,* 68**,** 797-807.

WANG, G., KONG, H., SUN, Y., ZHANG, X., ZHANG, W., ALTMAN, N., DEPAMPHILIS, C. W. & MA, H. 2004. Genome-wide analysis of the cyclin family in Arabidopsis and comparative phylogenetic analysis of plant cyclin-like proteins. *Plant Physiol,* 135**,** 1084-99.

WANG, R. & ESTELLE, M. 2014. Diversity and specificity: auxin perception and signaling through the TIR1/AFB pathway. *Curr Opin Plant Biol,* 21**,** 51-58.

WILLIAMS, J. H., TAYLOR, M. L. & O'MEARA, B. C. 2014. Repeated evolution of tricellular (and bicellular) pollen. *Am J Bot,* 101**,** 559-71.

WOJCIECHOWSKI, M. F., LAVIN, M. & SANDERSON, M. J. 2004. A phylogeny of legumes (Leguminosae) based on analysis of the plastid matK gene resolves many well-supported subclades within the family. *Am J Bot,* 91**,** 1846-62.

WUEST, S. E., VIJVERBERG, K., SCHMIDT, A., WEISS, M., GHEYSELINCK, J., LOHR, M., WELLMER, F., RAHNENFUHRER, J., VON MERING, C. & GROSSNIKLAUS, U. 2010. Arabidopsis female gametophyte gene expression map reveals similarities between plant and animal gametes. *Curr Biol,* 20**,** 506-12.

YAO, S., JIANG, C., HUANG, Z., TORRES-JEREZ, I., CHANG, J., ZHANG, H., UDVARDI, M., LIU, R. & VERDIER, J. 2016. The Vigna unguiculata Gene Expression Atlas (VuGEA) from de novo assembly and quantification of RNA-seq data provides insights into seed maturation mechanisms. *Plant J,* 88**,** 318-327.

YAO, X., TIAN, L., YANG, J., ZHAO, Y. N., ZHU, Y. X., DAI, X., ZHAO, Y. & YANG, Z. N. 2018. Auxin production in diploid microsporocytes is necessary and sufficient for early stages of pollen development. *PLoS Genet,* 14**,** e1007397.

ZHAN, J. P., THAKARE, D., MA, C., LLOYD, A., NIXON, N. M., ARAKAKI, A. M., BURNETT, W. J., LOGAN, K. O., WANG, D. F., WANG, X. F., DREWS, G. N. & YADEGARIA, R. 2015. RNA Sequencing of Laser-Capture Microdissected Compartments of the Maize Kernel Identifies Regulatory Modules Associated with Endosperm Cell Differentiation. *Plant Cell,* 27**,** 513-531.

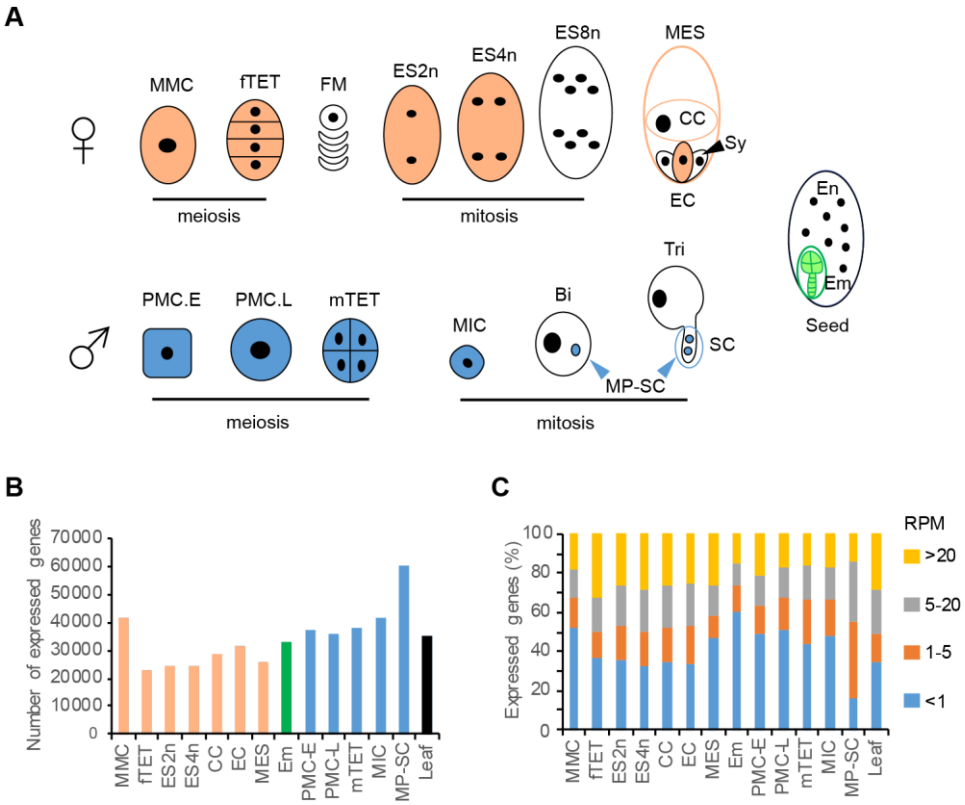

Figure 1. Stages of reproductive development in cowpea and gene expression in developed transcriptomes.

A, Cartoon of temporal stages of male and female gametophyte development showing cell-type stages collected by LCM for RNAseq. For detail refer to text. B, The number of genes expressed in each transcriptome set (RPM >0). C, The proportion of genes expressed at very low (<1RPM), low (1-5RPM), moderate (5-20RPM) or high (>20RPM) levels in RNAseq sets.

Abbreviations: MMC, megaspore mother cell; fTET, female tetrads; FM, functional megaspore selection stage (not collected); ES2n, mitotic embryo sac with 2 nuclei; ES4n, embryo sac with 4 nuclei; MES, mature embryo sac at anthesis, where antipodals have degenerated, containing the egg cell (EC), flanking synergids (Sy, not collected), and central cell (CC); Em, embryo; En, endosperm (not collected); PMC.E, early pollen mother cell; PMC.L, late pollen mother cell; mTET, male tetrads; MIC, uninucleate microspore; Bi, bicellular pollen stage; Tri, tricellular pollen stage, two sperm cells (SC) in the emerging pollen tube; MP-SC, mature pollen-sperm cell.

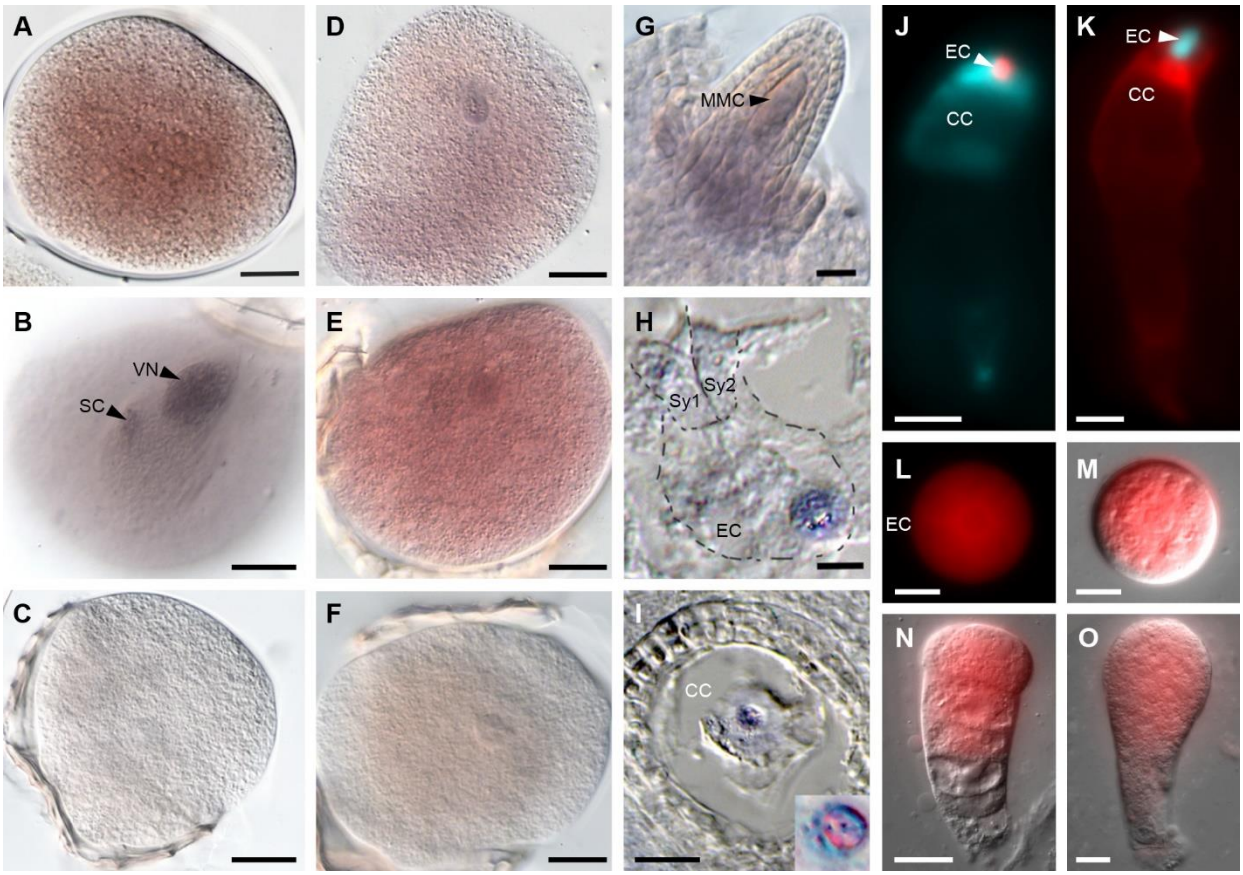

Figure 2. Gene expression in cowpea reproductive cell-types.
A – J, Whole-mount *in situ* hybridization (WISH) in pollen grains of cowpea using four different antisense probes. A-C, *VuXTH6* mRNA in sperm cells A and vegetative nucleus B, with no signal in the sense control C. D and E, *VuXTH32* was detected in sperm cell and vegetative cell cytoplasm. F, *VuXTH32* sense controls. G, Whole-mount ovule undergoing megasporogenesis showing *VuKNU1* mRNA localized in the MMC, the nucellus and the initial inner integument. H, Paraffin section through a differentiated female gametophyte showing *VuRKD1* mRNA localization in the egg cell and synergids. I, Paraffin section through a differentiated female gametophyte showing *VuNB-ARC* mRNA localization in the central cell. Inset shows fused polar nuclei showing active transcription of *VuNB-ARC*. J, $AtRKD2_{pro}$:*dsRED-Express* (red) in EC and $AtDD9_{pro}$:*AmCyan1* (cyan) in CC one day before anthesis. K, $AtEC1.1_{pro}$:*AmCyan1* (cyan) in EC and $AtDD25_{pro}$:*dsRED-Express* (red) in CC. L-M, $AtDD45_{pro}$:*dsRED-Express* (red) in isolated egg cell, N, two-celled proembryo and O, early embryo.
Abbreviations: EC, egg cell; CC, central cell; Sy, synergids; SC, sperm cells; VN, vegetative nucleus, MMC, megaspore mother cell.
Scale bars: A-G, L-M = 10 µm, H = 8 µm, I = 14 µm, J-K = 50 µm, N-O = 20 µm.

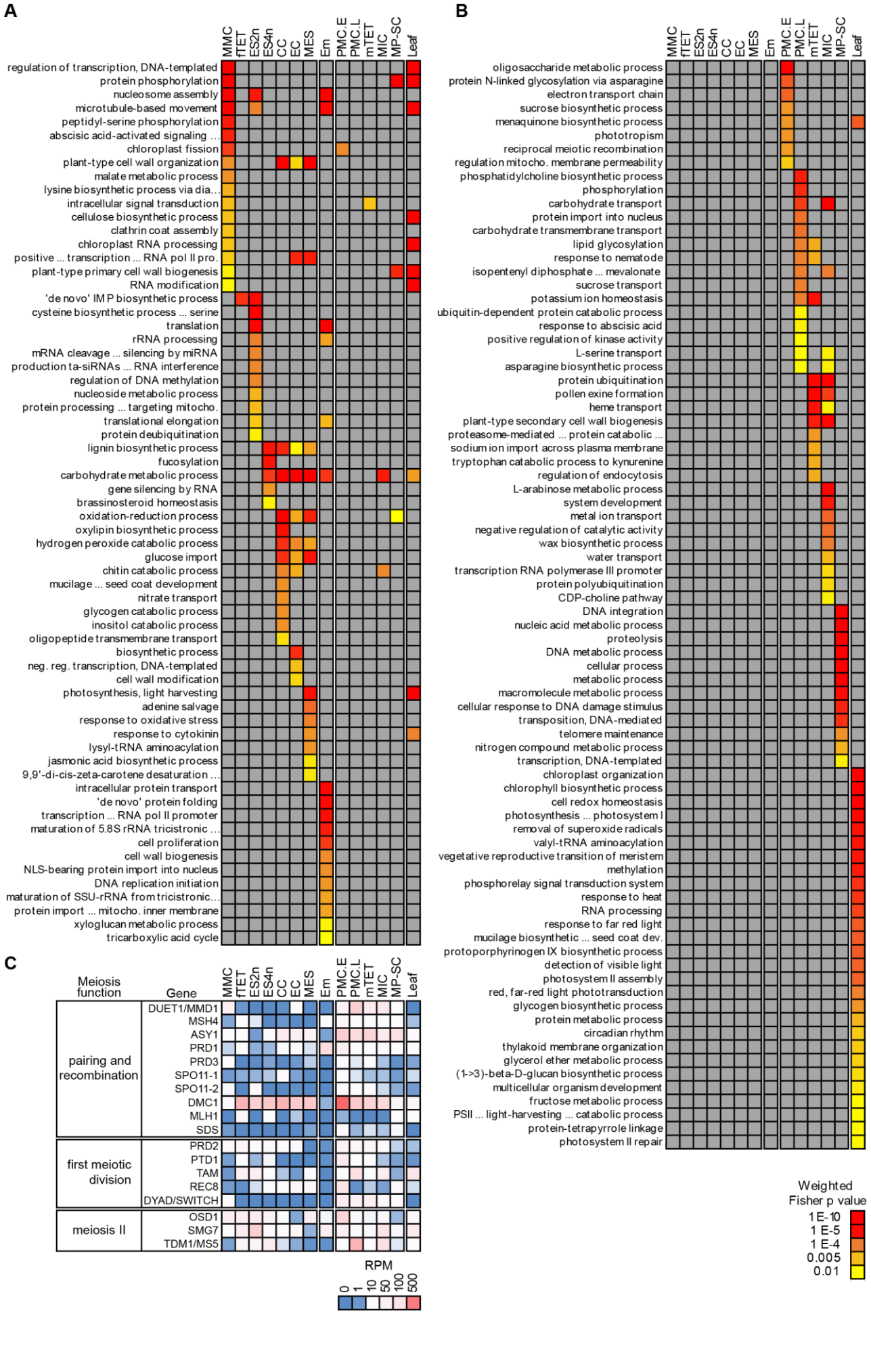

Figure 3. Differentially enriched Biological Process GO terms and expression of meiosis genes during gametogenesis.

A, Enriched GO terms primarily in female gametophyte and early embryo transcriptomes. B, Enriched GO terms primarily in the male gametophyte and leaf transcriptomes. The statistical significance of the GO enrichment is represented according to the scale of weighted Fisher p value shown at the bottom right. C, Expression of genes involved in meiosis in the generated cowpea transcriptomes (see also Supplemental Tables 7 and 8). Expression levels relate to the RPM scale.

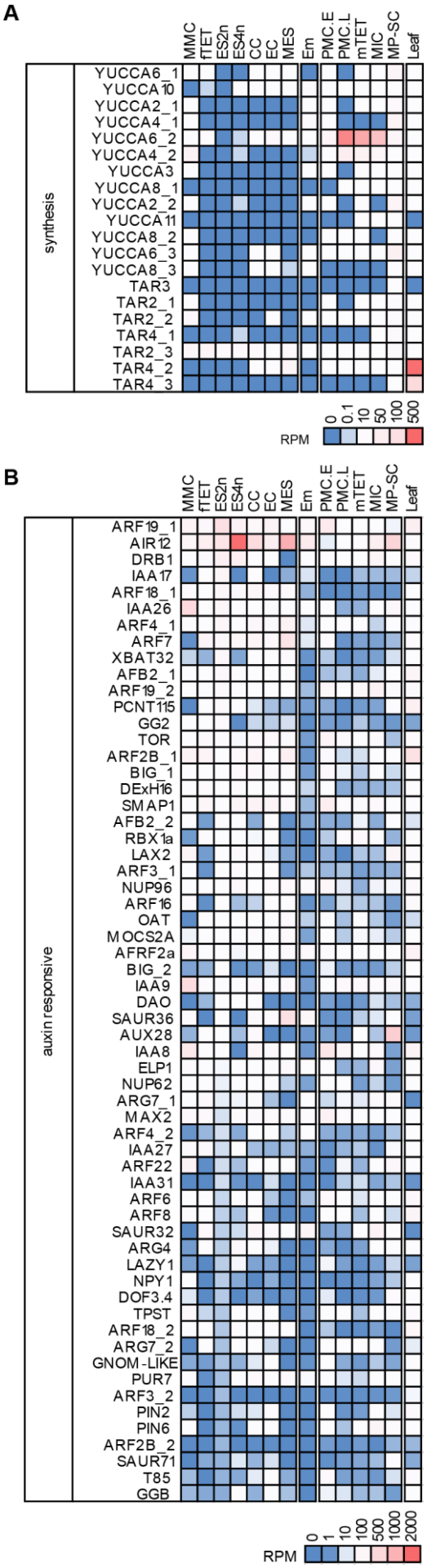

Figure 4. Expression of auxin biosynthesis and auxin responsive genes during meiosis and gametophyte development.
A, Expression of genes belonging to the YUCCA and TAR auxin biosynthesis gene families. B, Expression of 60 auxin responsive genes sorted in decreasing order of expression level in the 2-nucleate embryo sac. Expression levels are related to the RPM scale with each respective panel (see also Supplemental Table 9).

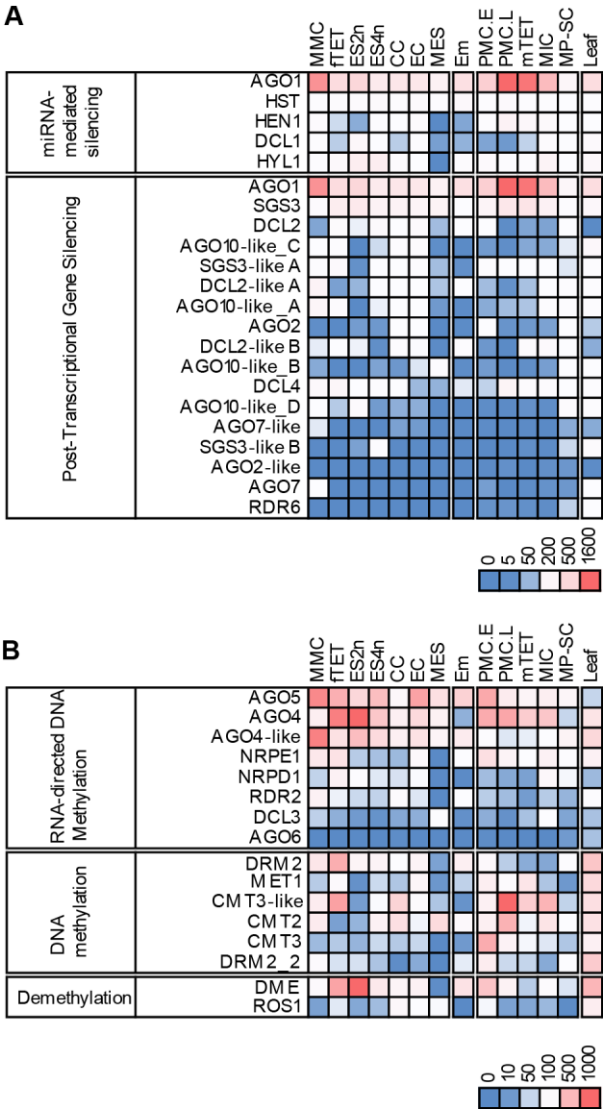

Figure 5. Heatmaps representing the expression of selected genes involved in RNA-mediated gene silencing and DNA methylation.

A, Expression of genes involved in the miRNA-mediated gene silencing pathway and involved in PTGS. B, Expression of genes that interact with RNA and are involved in RdDM, DNA methyltransferases that mediate RdDM and DNA glycosylases that mediate demethylation of DNA. Expression level is according to the RPM scales with each panel (see also Supplemental Tables 12 and 13).

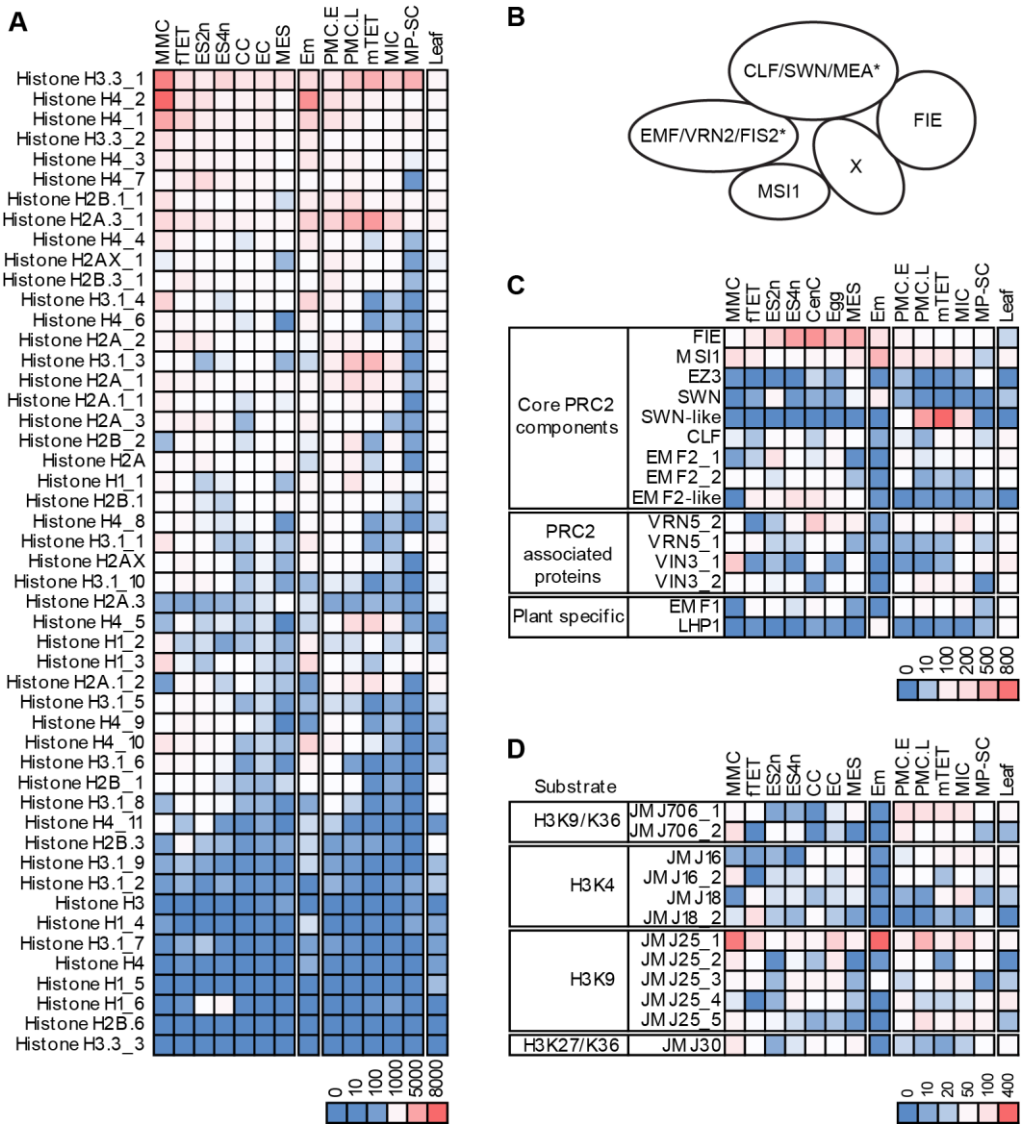

Figure 6. Histone gene expression and the expression of selected genes involved in histone modification.

A, Expression of genes belonging to the core histone family (see Supplemental Table 18). B, Expression of selected PcG genes involved in histone methylation resulting in gene silencing (see Supplemental Table 19). C, Known protein interactions forming Polycomb-group repressive 2 complex types. Accessory proteins (X) are often associated with PRC2 complex function. Asterisks indicate *Arabidopsis* specific proteins. MEA and *Arabidopsis* counterparts, SWN and CLF are SET domain protein and homologs of *Drosophilia* Enhancer of Zeste. FIS2 and others listed are VEFS-box proteins. FIE and MSI1 are WD40 repeat protein containing proteins (Mozgova and Henning, 2015). D, Expression of selected JMJ family histone demethylase genes and demethylation targets, at left (see also Supplemental Tables 14, 15, 16). Expression levels relate to the RPM scales associated with each panel.

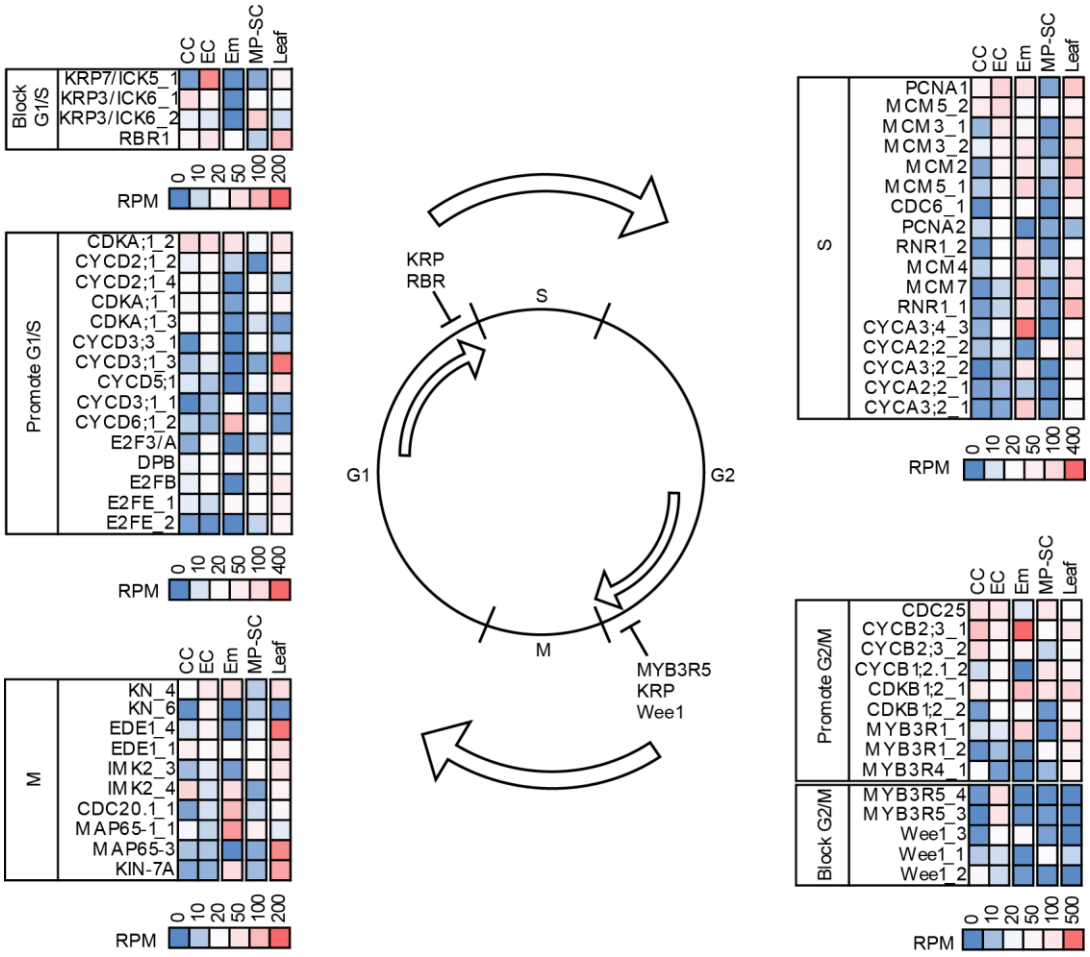

Figure 7. Expression of selected cell cycle genes in egg, central cell, mature pollen-sperm and leaf transcriptomes.

Cell cycle genes are grouped according to their function in the cell cycle relating to roles in promoting or blocking progression through various cell cycle phases. Relative expression level is indicated according to the RPM scale shown at the bottom of each panel (see also Supplemental Tables 10 and 11).

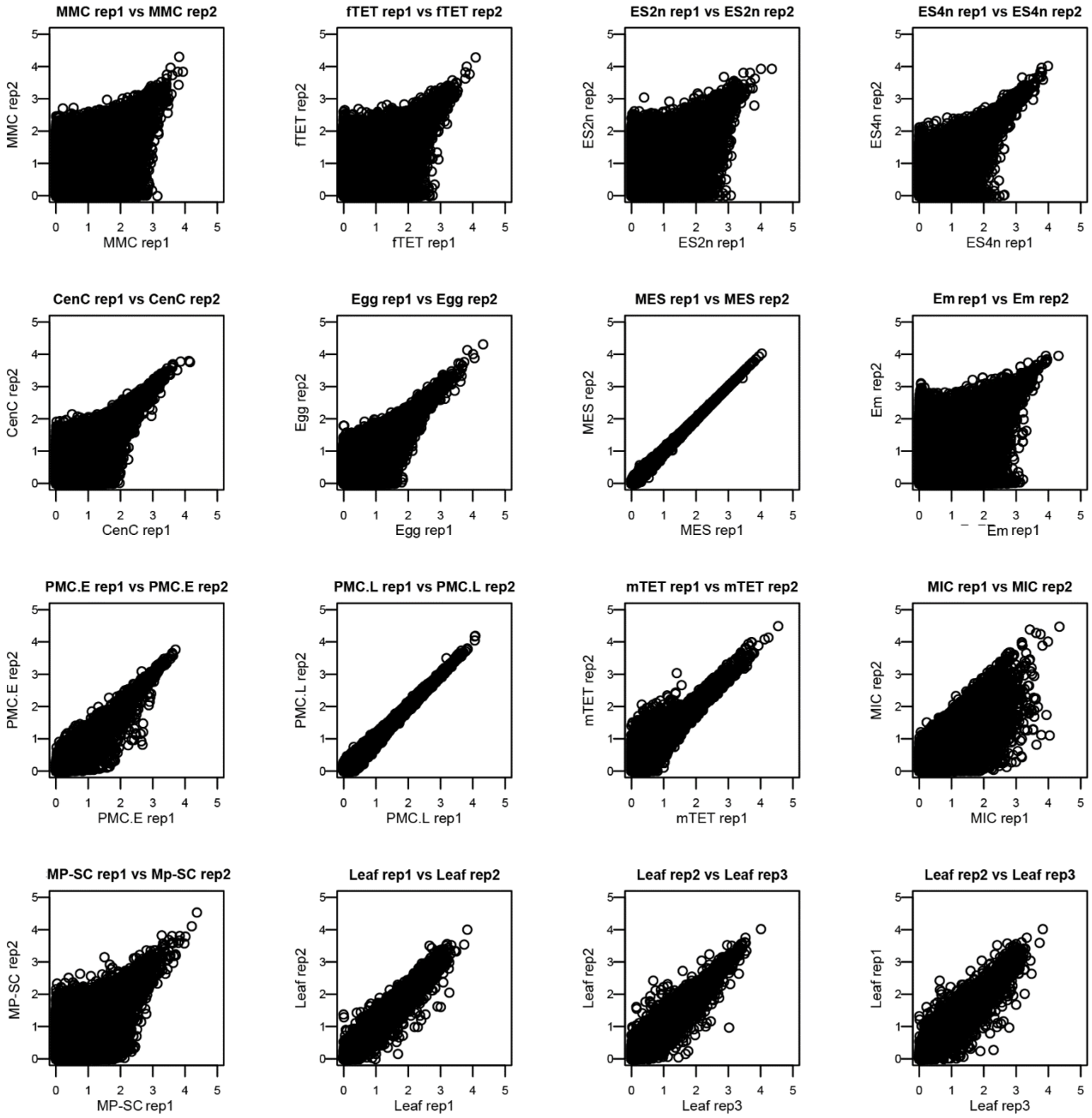

Supplemental Figure 1. Correlation between RNAseq replicates.
Scatter plot of log-transformed mean RPM counts of replicates for each tissue. Replicate 1 and replicate 2 for each cell-type are shown on the Y and X axes, respectively.

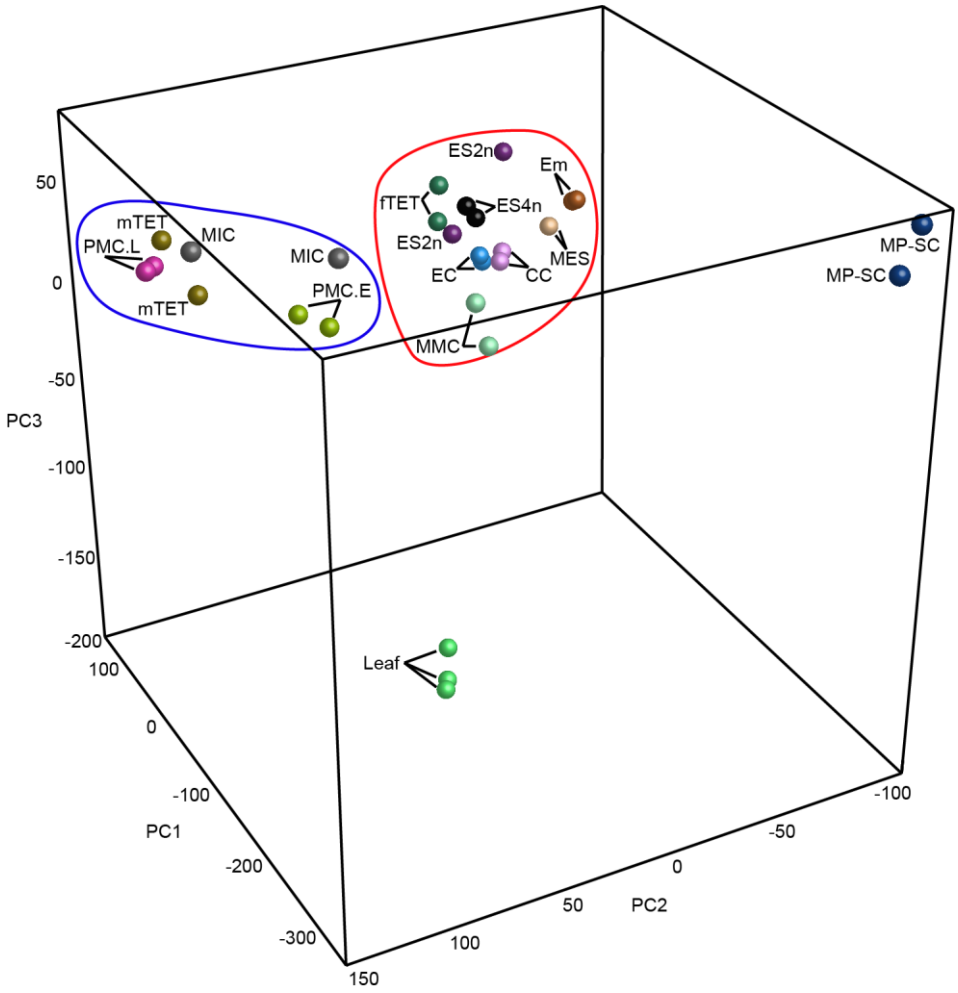

Supplemental Figure 2. Principal component analysis (PCA).
PCA plot showing relationships between all transcriptomes.
Abbreviations: MMC, megaspore mother cell; fTET, female tetrads; ES2n, mitotic embryo sac with 2 nuclei; ES4n, embryo sac with 4 nuclei; MES, mature embryo sac at anthesis, containing the egg cell (EC) and central cell (CC); Em, embryo; PMC.E, early pollen mother cell; PMC.L, late pollen mother cell; mTET, male tetrads; MIC, uninucleate microspore; MP-SC, mature pollen-sperm cell.

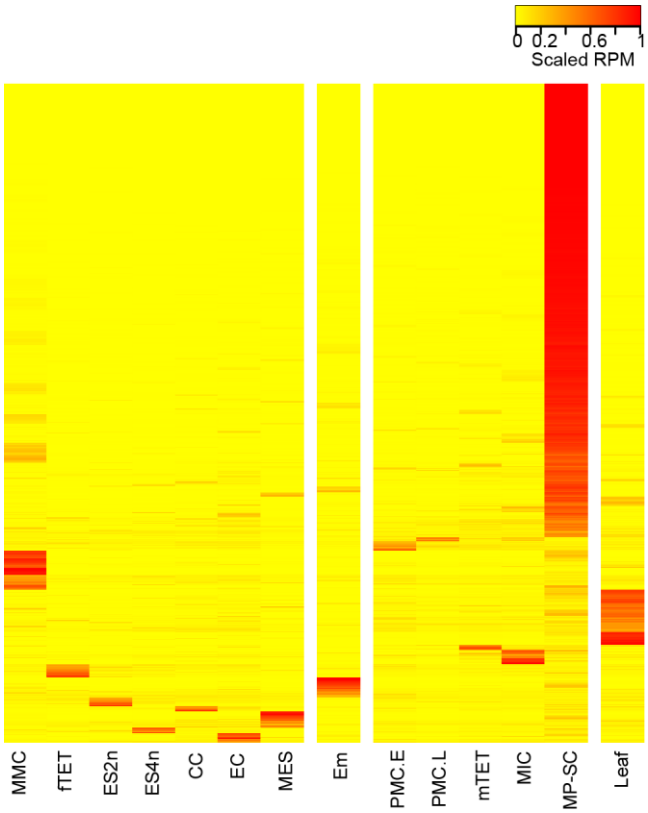

Supplemental Figure 3. Cell-specific genes expression.
Heat-map of scaled RPM expression values of the cell-specific genes identified by using the rsgcc software package.

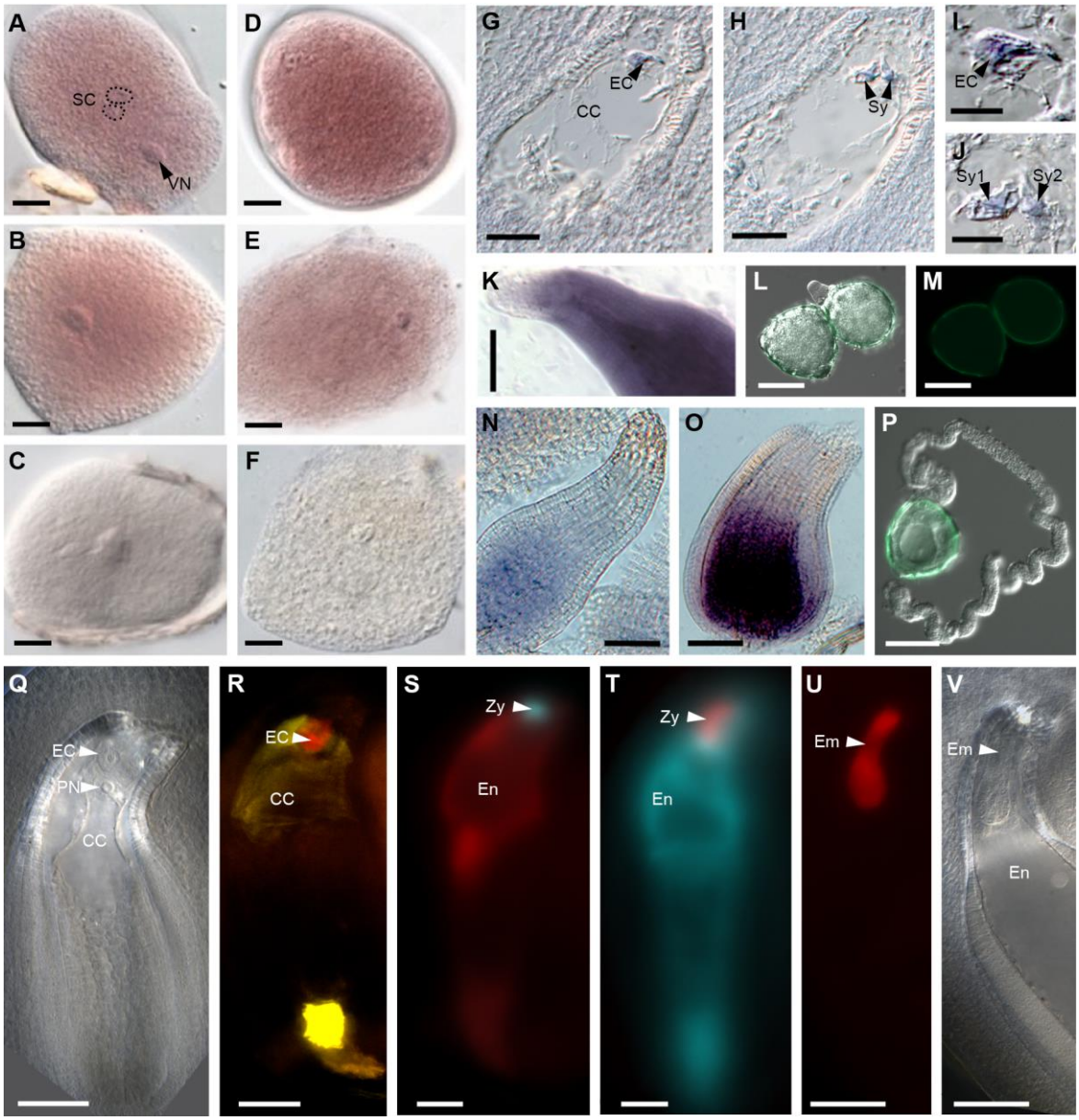

Supplemental Figure 4. *In situ* hybridization of cell-specific cowpea genes in gametophytic tissue and fluorescent reporters expressed from *Arabidopsis* cell-specific promoters in cowpea. A-B, *VuXTH32* mRNA localized in the sperm cells and vegetative cell cytoplasm. C, *VuXTH32* sense control. D-E, *VuAt3g09950* mRNA abundantly localized in the sperm and vegetative cells. F, sense *VuAt3g09950* control. G, Paraffin section through a fully differentiated female gametophyte showing *VuEC1.1* mRNA localization in the egg cell. H, Consecutive section to (G) showing *VuEC1.1* mRNA localization in the synergids. I, Detail of G showing mRNA localization in the egg cell. J, Detail of H showing mRNA localization in the synergids. K, Whole-mounted ovule showing *VuMEE23* mRNA localization in the central cell and adjacent nucellar cells. L-M, $AtDUO1_{pro}$*:AcGFP1* no expression. N, Whole-mounted ovule showing *VuSDR1* mRNA localization in the central cell. O, Whole-mounted ovule showing *VuGULL06* mRNA localization confined to the central cell. P, No expression of $AtLAT52_{pro}$*:AcGFP1* in germinating pollen. Q, Mature female gametophyte with egg cell, polar nuclei and central cell in cleared ovule. R, $AtDD45_{pro}$*:dsRED-Express* (red) in EC and general pattern of the $AtDD1_{pro}$*:ZsYellow1* (yellow) in cells external to the embryo sac and in CC. S, $AtEC1.1_{pro}$*:AmCyan1* (cyan) in zygote and $AtDD25_{pro}$*:dsRED-Express* (red) in early endosperm. T, $AtRKD2_{pro}$*:dsRED-Express* (red) in zygote and $AtDD9_{pro}$*:AmCyan1* (cyan) in early endosperm. U, $AtRKD2_{pro}$*:dsRED-Express* in early embryo. *AtDD9* is not expressed at this stage. V, Cleared ovule showing early embryo corresponding to the stage in U.

Scale bars: A-F, I-J = 10 µm; G-H = 18 µm; K, N-O = 35 µm; L-M, P-T = 50 µm; U-V = 100 µm

Abbreviations: EC, egg cell; CC, central cell; Sy, synergids; SC, sperm cells; VN, vegetative nucleus; PN, polar nuclei; Em, embryo; En, endosperm; Zy, zygote.

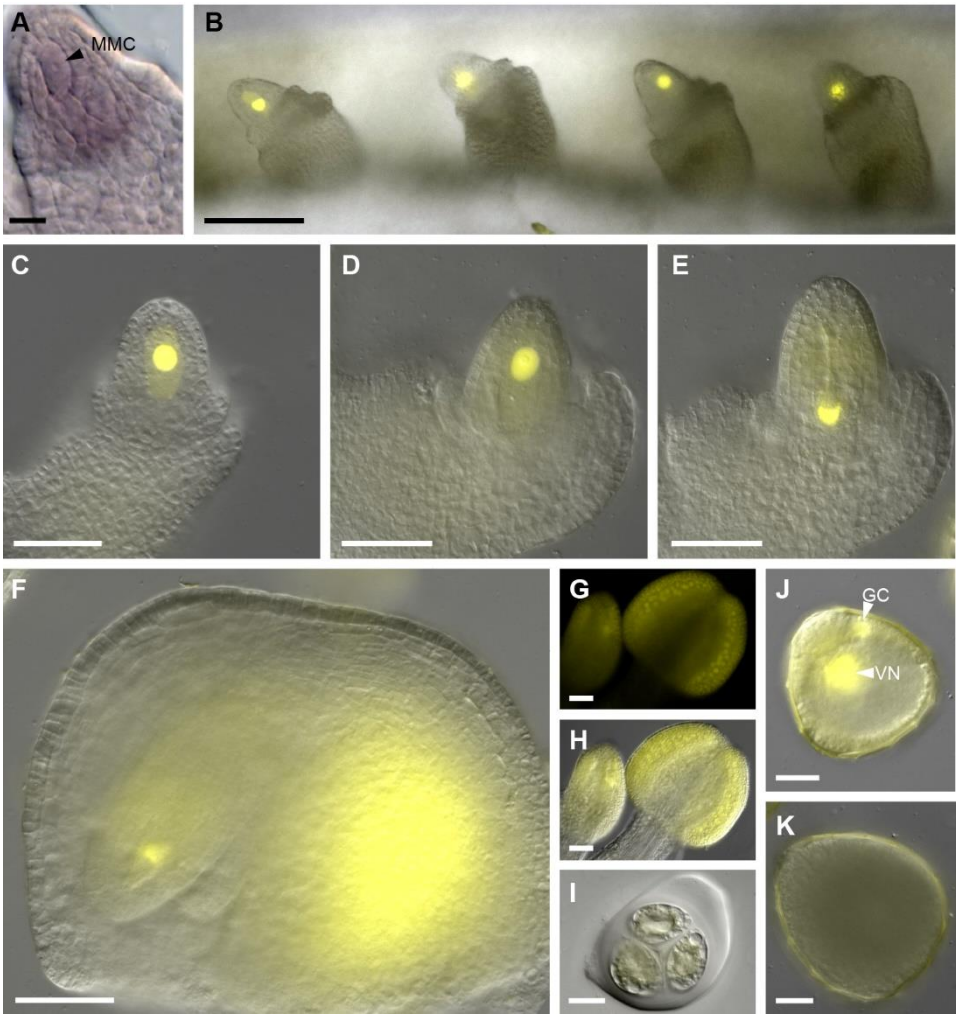

Supplemental Figure 5. Expression of the *KNU* genes in cowpea.
A, Whole-mount pre-meiotic ovule showing *VuKNU1* mRNA localized in the MMC and the developing nucellus at the onset of integument initiation. B-D, Micrographs of cowpea ovules expressing a *AtKNU*$_{pro}$*:nlsYFP* reporter construct marking MMC fate. E-F, At the end of meiosis *KNU* promoter turns off in female functional megaspore, but the expression persists in somatic ovule cells at the chalazal end. G-H, Expression of *AtKNU*$_{pro}$*:nlsYFP* reporter construct during male meiosis. I, Male tetrad showing no expression of reporter construct. J, After the first pollen mitosis, the expression of reporter construct is evident in both vegetative and generative nuclei. K, Mature pollen grain does not show any expression.
Abbreviations: MMC, megaspore mother cell; GC, generative cell; VN, vegetative nucleus. Scale bars: A = 10 µm; B = 100 µm; C-H = 50 µm; I-K = 20 µm.

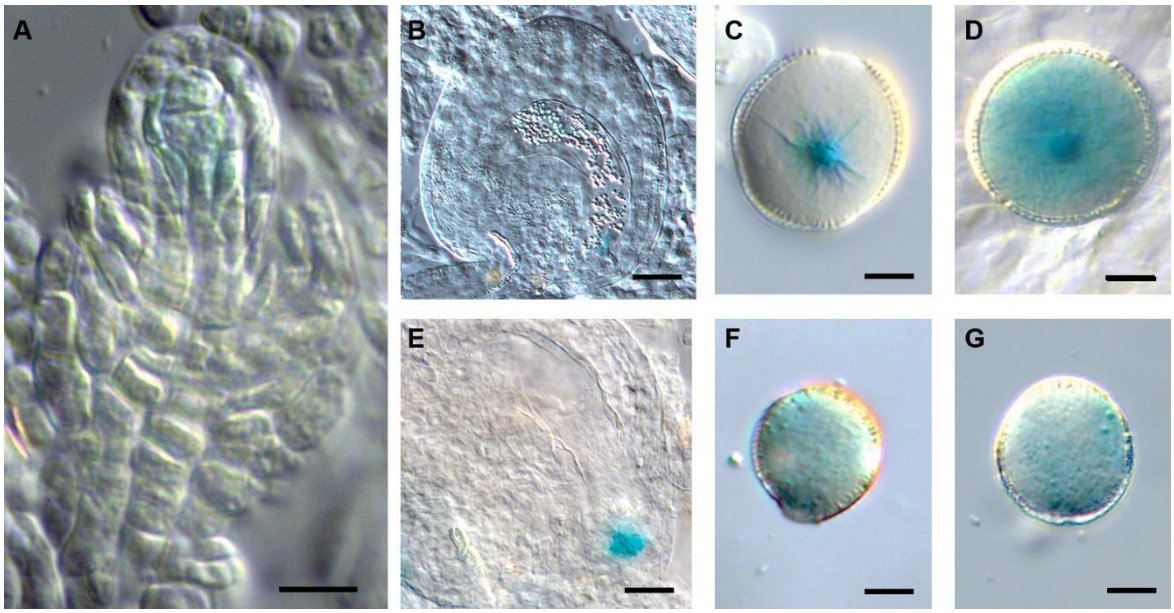

Supplemental Figure 6. Specific activity of cowpea promoters in reproductive cells of *Arabidopsis thaliana*.

A, *VuKNU-L1*$_{pro}$*:GUS* expression in the developing ovule of *Arabidopsis*. B, *VuRKD1*$_{pro}$*:GUS* expression in the egg cell. C, *VuRKD1*$_{pro}$*:GUS* expression in a sperm cell. D, *VuRKD1*$_{pro}$*:GUS* expression in the vegetative cell. E, *VuGULL06*$_{pro}$*:GUS* in the egg apparatus. F, *VuXTH32*$_{pro}$*:GUS* expression in the vegetative cell. G, *VuGIM2*$_{pro}$*:GUS* expression in the vegetative cell. Scale Bars: A, F and G = 10 µm; B and E = 20 µm; C and D = 8 µm.

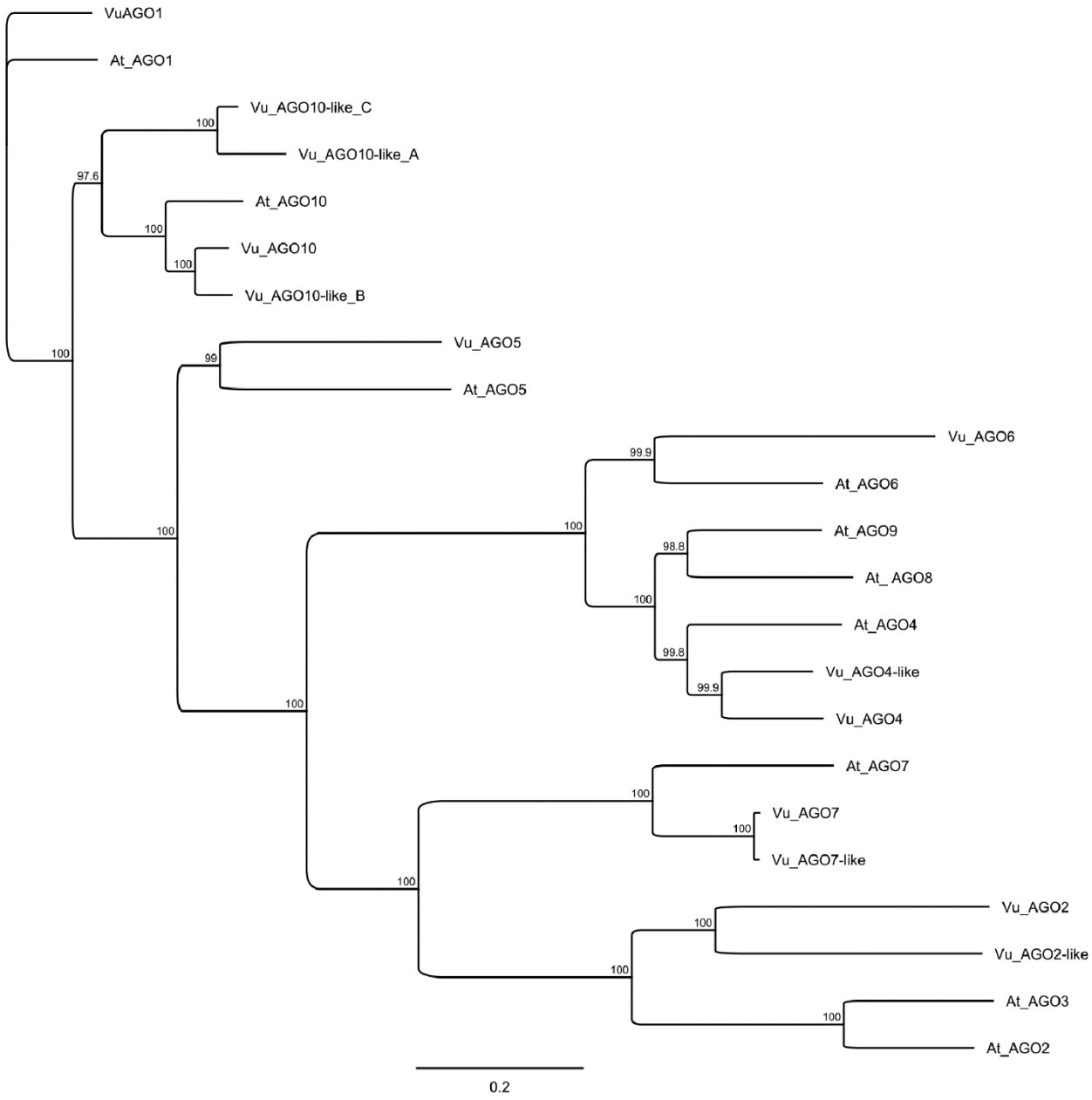

Supplemental Figure 7. Phylogeny of the AGO family in cowpea and *Arabidopsis.*
A Jukes-Cantor Neighbour-Joining consensus tree showing the relationship between the AGO genes identified in cowpea (Vu) and those known in *Arabidopsis* (At).
Parameters for tree building were ClustalW MSA with BLOSUM cost matrix, Gap open cost 10, Gap extend cost 0.1. Jukes-Cantor Neighbour-Joining consensus tree, no outgroup, Bootstrap resampling with 1000 replicates, 50% support threshold.

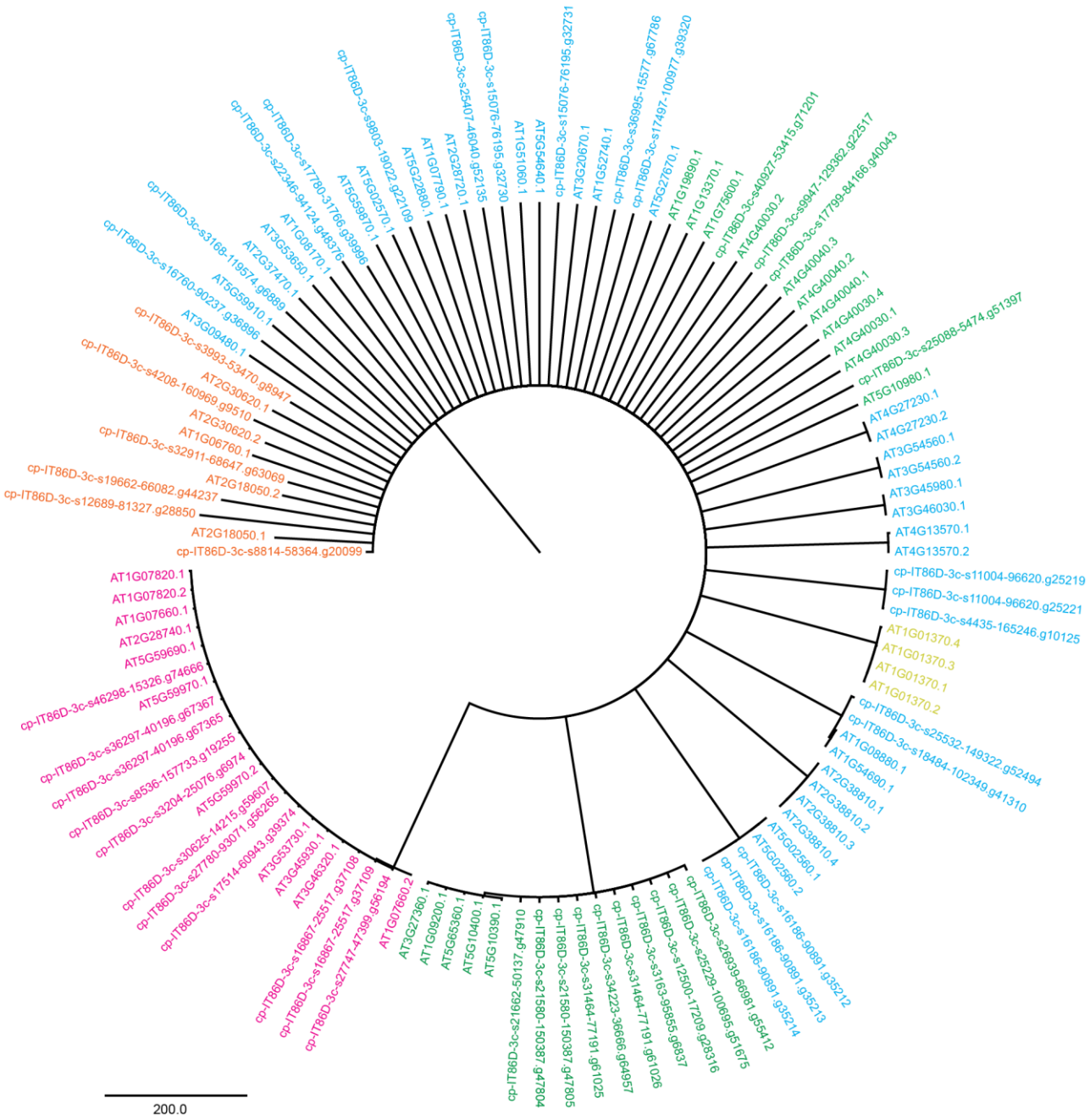

Supplemental Figure 8. Phylogeny of *Arabidopsis* and cowpea histone proteins.
Jukes-Cantor Neighbour-Joining consensus tree showing the relationship between the *Arabidopsis* and cowpea histones is shown. Histone1 (orange), Histone2 (blue), Histone3 (green), Histone4 (pink), CenH3 (yellow). A Parameters for tree building were ClustalW MSA with BLOSUM cost matrix, Gap open cost 10, Gap extend cost 0.1. Jukes-Cantor Neighbour-Joining consensus tree, no outgroup, Bootstrap resampling with 1000 replicates, 50% support threshold.